1965

Order-disorder in Fe_3Al at various temperatures induced by neutron irradiation

Robert F. Toma Jr.

ORDER-DISORDER IN Fe_3Al AT VARIOUS TEMPERATURES INDUCED BY NEUTRON IRRADIATION

BY

ROBERT F. TOMA JR.

- - - - - - - - - -

A

THESIS

submitted to the faculty of the

UNIVERSITY OF MISSOURI AT ROLLA

in partial fulfillment of the work required for the

Degree of

MASTER OF SCIENCE IN METALLURGICAL ENGINEERING

Rolla, Missouri

1965

- - - -

Approved by

Advisor

ABSTRACT

Resistivity measurements were made on ordered and disordered Fe_3Al samples while irradiated by neutrons.

In the ordered as well as the disordered state, the different Fe_3Al samples were heated to 100, 150, 200, 250, and 300°C respectively, and were irradiated by a fast neutron flux of 0.534×10^{10} neutrons/cm^2-sec. The ordered Fe_3Al measurements were characterized by an increase in resistivity denoting an advancement toward disorder. The disordered Fe_3Al measurements were characterized by a decrease in resistivity denoting an advancement toward order. In the Fe_3Al ordered and disordered samples irradiated at 300°C, the resistivities tended to become constant as the fast neutron flux reached 19.2×10^{13} neutrons/cm^2. This indicated that the amount of disordering is in equilibrium with the amount of ordering, and that the relatively high temperature of 300°C is the cause for this. The other ordered and disordered Fe_3Al samples irradiated at lower temperatures did not show this effect when the fast neutron flux reached 19.2×10^{13} neutrons/cm^2. If these samples had continued to be neutron irradiated, they too, at some higher flux, would have experienced this effect of the amount of disordering approximately equaling the ordering.

Two different long range order parameters were obtained for both the ordered and disordered Fe_3Al samples.

Resistivity measurements were used to calculate one of the parameters. In this case, the resistivity at the elevated temperature was used. The second long range order parameter was obtained by integrated intensities of the x-ray diffraction pattern. In this case, the order parameter was obtained for room temperature. It was found that the parameter obtained by the integrated intensity method, for both ordered and disordered samples, was substantially larger than the one obtained by using the resistivity method. This indicated that the point defects produced during irradiation were annealed as the Fe_3Al samples were cooled from the test temperature to room temperature.

ACKNOWLEDGEMENTS

The author wishes to express his appreciation to Dr. H. P. Leighly Jr., Associate Professor of Metallurgical Engineering, for his valuable assistance and guidance throughout this very interesting investigation.

He also wishes to extend his gratitude to Dr. D. R. Edwards, Director of the Nuclear Reactor, for valuable suggestions and cooperation.

The iron-aluminum alloy used in this investigation was supplied by the Naval Ordnance Laboratory.

I would also like to thank the National Science Foundation under whose traineeship I was able to do my investigation.

TABLE OF CONTENTS

LIST OF FIGURES

LIST OF TABLES

CHAPTER I

INTRODUCTION

A. Radiation effects on order and disorder.

It is usually necessary to conduct an investigation of the nature of neutron radiation damage in solids either on alloys having a peculiarity of value for the study of the action of irradiation, or on well studied pure metals.

These alloys include ordered alloys (superlattice structure), which are characterized by an ability for regular distribution of the component atoms at preferred points of the crystal lattice. It is convenient to study radiation effects on ordered and disordered alloys for two reasons. It should be pointed out that certain physical properties of superlattice structures vary within considerable limits when they pass from a disordered to an ordered distribution of atoms(and vice versa). In the first place, ordered and disordered alloys are very sensitive to irradiation by neutrons, which permits a quantitative study of radiation effects. In the second place, any exchange of position by alloy atoms, a process that remains unnoticed in normal alloys and pure metals, such as the return of atoms displaced into the interstices back to the lattice points, leads to a change in the degree of order or disorder. Consequently, a change in the properties of the ordered or disordered alloy is observed.

A study of the action of neutron irradiation on ordered and disordered alloys is also of interest from the point of view of investigating the very process of the order-disorder transformation.

B. Resistivity.

Quantum mechanical treatments of the electrical conductivity of alloys leads to the conclusion that a perfectly periodic structure would have zero resistance and that the finite resistance of alloys is due to departures from perfect periodicity(12). It is to be expected that the presence or absence of order, being associated with the presence or absence of a regular arrangement of the constituent atoms of an alloy, will have a pronounced effect on the resistivity of an alloy. The results of investigations to determine the variation of resistivity with neutron irradiation and temperature in Fe_3Al are described in Chapter IV. Attempts to correlate neutron radiation damage with degree of long range order in Fe_3Al are also reported.

CHAPTER II

REVIEW OF LITERATURE

The following is a review of the investigations on Fe_3Al which are pertinent to the specific problems of the present study, namely the superlattice encountered, the electrical resistivity of Fe_3Al as a function of the temperature and fast neutron irradiation, and measurement of long range order as a function of temperature and fast neutron irradiation.

A. Explanation of the term superlattice.

A crystal is composed of atoms arranged in a regular three dimensional array. Since the array is regular, in order to specify a structure it is not necessary to indicate the positions of all the atoms. It is necessary only to specify that group of atoms which is repeated to form the whole crystal together with the three units of translation. If these units of translation are applied to a single point, the lattice of the crystal is produced which is the framework without the atoms. The figure of which the three units of translation are the edges is called the unit cell, and a unit cell can be found by joining any one atom to the three nearest atoms that are similar and have similar enviroments, provided that the four atoms are not in the same plane.

The term lattice is used to represent the complete structure, whereas, it is an abstraction useful only in

describing structures. The error has arisen because many metallic structures can be completely specified by placing the same atoms at each point of the lattice. For example, copper has its atoms arranged on the points of a face-centered cubic lattice, and α-iron has its atoms arranged on the points of a body-centered cubic lattice. These lattices are both formed by equal, mutually perpendicular, translations, but the copper has extra lattice points at the centers of the faces of the unit cells, and the iron has an extra point at the center of gravity of the unit cell.

This concept is satisfactory for pure metals, but requires modification for solid solutions. Suppose there is a solid solution of 20 percent of element B in element A. If a B atom is placed at the lattice point, the lattice translations may not lead to a B atom. For solid solutions, therefore, the lattice is regarded as a collection of atomic sites. Whether an A atom or a B atom occupies a particular site depends upon several factors, the chief of which may be pure chance. Thus it is assumed that the atoms are arranged at random.

There is another point to be remembered. If the two atoms are of different sizes they will tend to displace each other from the lattice points, and the structure will not be quite regular. This factor is important in the theory of superlattice formation.

In many alloy systems, chance appears to be the main factor in deciding the apportionment of the atom. This is not always the case, for there may be a particular reason why dissimilar atoms tend to avoid or attract each other. If, in a binary alloy, dissimilar atoms avoid each other, a two phase system will be formed. If they attract, a superlattice structure will be formed(17). If in an alloy of equal atomic proportions, the presence of one type of atom on a lattice point demands that each neighboring point shall be occupied by an atom of the other type, the structure shown in Figure 1 is obtained. A corresponding structure with random distribution of atoms is shown in Figure 2.

The structure shown in Figure 1 is said to be ordered, and that shown in Figure 2 is said to be disordered. The former may also be said to be a superlattice structure, the term originating in the following way. To find the unit cell of the disordered structure, nearest atomic sites are joined as shown in Figure 2. Similar atoms cannot be joined, but with the ordered structure similar atoms can be joined as shown in Figure 1. This leads to a larger unit cell with axes inclined 45° to those of the disordered unit cell. If the directions of the axes of the disordered unit cell are to be retained, a centered cell which is still larger may be chosen. These larger unit cells, which are derived from smaller

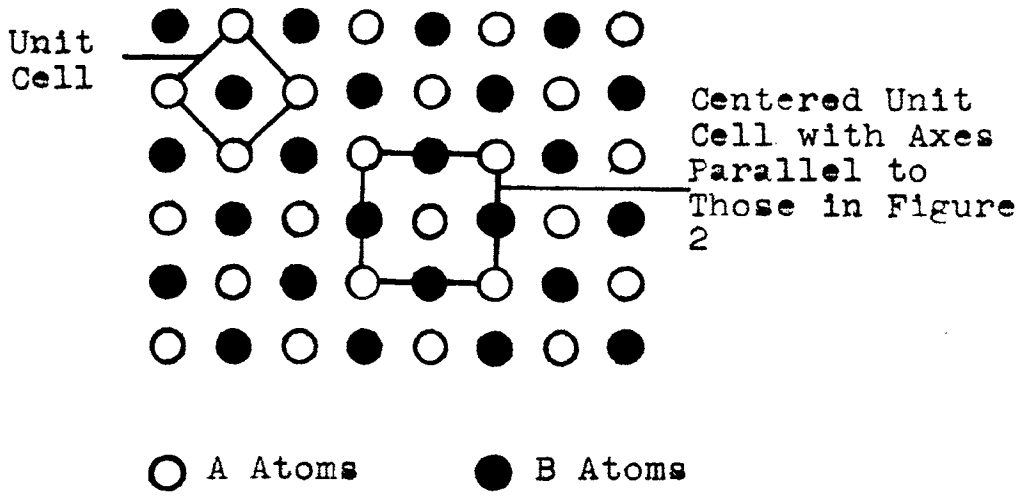

Superlattice Structure of Composition AB.

Figure 1.

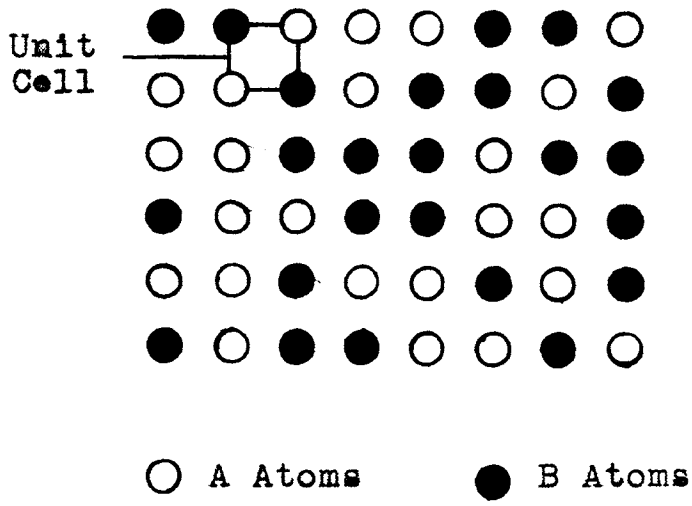

Disordered Solid Solution of Composition AB.

Figure 2.

ones, leads to the name superlattice(17).

The formation of the perfect superlattice occurs at relatively low temperatures. Therefore, in order for a superlattice to form, the ordered arrangement of atoms must be more favored energetically than the random distribution (attraction between unlike atoms must be greater than attraction between like atoms). As the temperature increases, the amplitudes of the thermal vibrations of atoms about their equilibrium positions will become greater and pairs or small groups of atoms will acquire sufficient energy to break away from their original places in the lattice and exchange positions. Therefore, according to free energy considerations, at high temperatures, the disordered arrangement of atoms will become more stable than the ordered one. Thus, we expect a transition temperature at which the superlattice ceased to be stable. This temperature is called the critical temperature for the order-disorder transformation. The critical temperature for Fe_3Al is about $540^{\circ}C$(23).

According to the above considerations, some kind of thermodynamic equilibrium distribution of atoms over lattice points of the alloy will be expected to exist at each temperature after suitable heat treatment. As stated earlier, the extreme cases are the perfectly ordered distribution at very low temperatures and the disordered one above the critical temperature. Between these two ex-

tremes, any intermediate state is possible at corresponding temperatures. This behavior is in marked contrast to that of transitions between liquid and solid in which the substance does not pass through intermediate states.

In order to specify the degree of order of the arrangement of atoms over lattice points in any state mentioned above, an order parameter necessary for a theoretical understanding of the mechanism of the transition from the ordered to the disordered state in Fe_3Al will be introduced. Such a parameter is called a long range order parameter, S, which was introduced by Bragg and Williams(5).

When the perfectly ordered arrangement of atoms in binary alloys is realized, the lattice points occupied by A atoms will be called α sites and those by B atoms will be called β sites. If a binary alloy of AB having a body centered cubic structure is considered, the positions on cube corners of a unit cell become α sites and those on cube centers become β sites. Let the total number of atoms, which is also the total number of sites, be N. Then F_A shall denote the fraction of A atoms, and $F_B = 1 - F_A$ the corresponding quantity for B atoms. Next, the fraction of α sites occupied by A atoms(right atoms) is r_α. The fraction of α sites wrongly occupied by B atoms is $w_\alpha = 1 - r_\alpha$. Similarly r_β and $w_\beta = 1 - r_\beta$ represents the rightly and wrongly occupied β sites respectively. The number of A atoms on β sites is

$w_\beta F_B N$ and is equal to the number of B atoms on α sites, $w_\alpha F_A N$. Then the Bragg-Williams order parameter or long-range order S may be written as

$$S = \frac{r_\alpha - F_A}{1 - F_A} = \frac{r_\beta - F_B}{1 - F_B} \qquad \text{(equation 1)}$$

which is defined so that it is unity for perfect order and zero for the disordered state.

On the basis of the work of Bradley and Jay(4), Hansen and Anderko(14) proposed for the solid solution region in Fe-Al alloys the phase diagram illustrated in Figure 3. In the phase field α'', a DO_3 superlattice based on the stoichiometric Fe_3Al exists. This structure is shown in Figure 4.

Recently Taylor and Jones(29) made precision lattice parameter measurements over a broad range of temperatures and compositions. They deduced the phase boundaries from discontinuities in the slopes of the isothermal plots of lattice parameters vs. composition. Their investigation confirmed the superlattice configuration proposed by Bradley and Jay.

McQueen and Kuczynski(20) have proposed an equilibrium diagram based on differential dilatometric heating curves of several alloys. Figure 5 indicates the phase limits determined by McQueen's and Taylor's investigations.

Sykes and Banpfylde(28) found that alloys containing from 12 to 16 atomic percent aluminum underwent a remark-

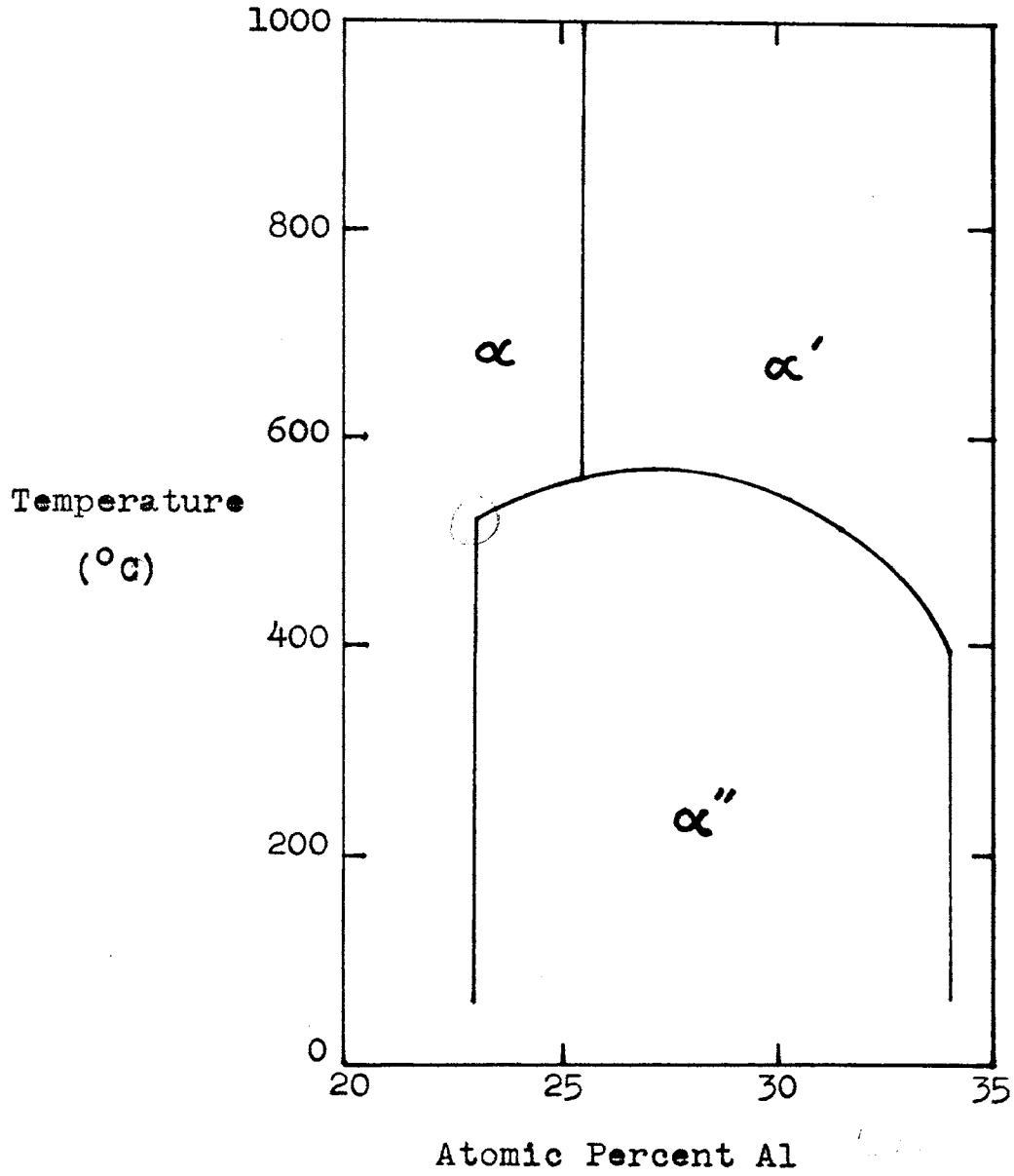

Iron-Aluminum Equilibrium Diagram.
Determined by Hansen and Anderko(14).
Figure 3.

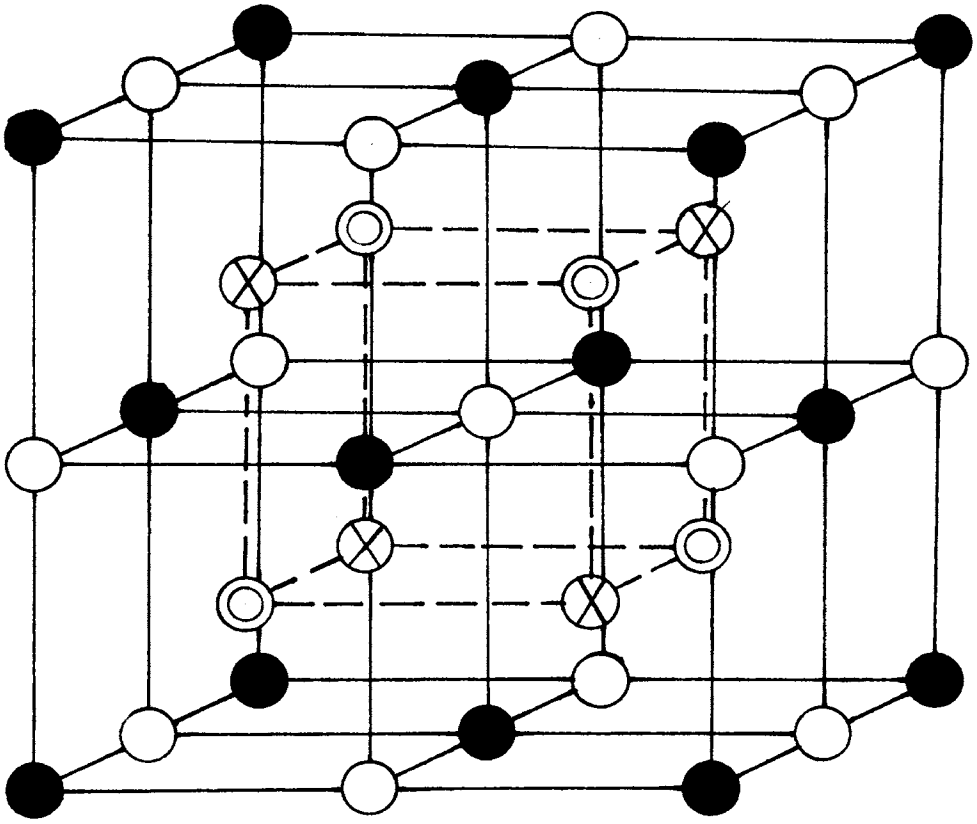

Fe_3Al: ○ ● ◎Fe ⊗Al

$Fe_3Al(DO_3)$ Superlattice(17)

Figure 4.

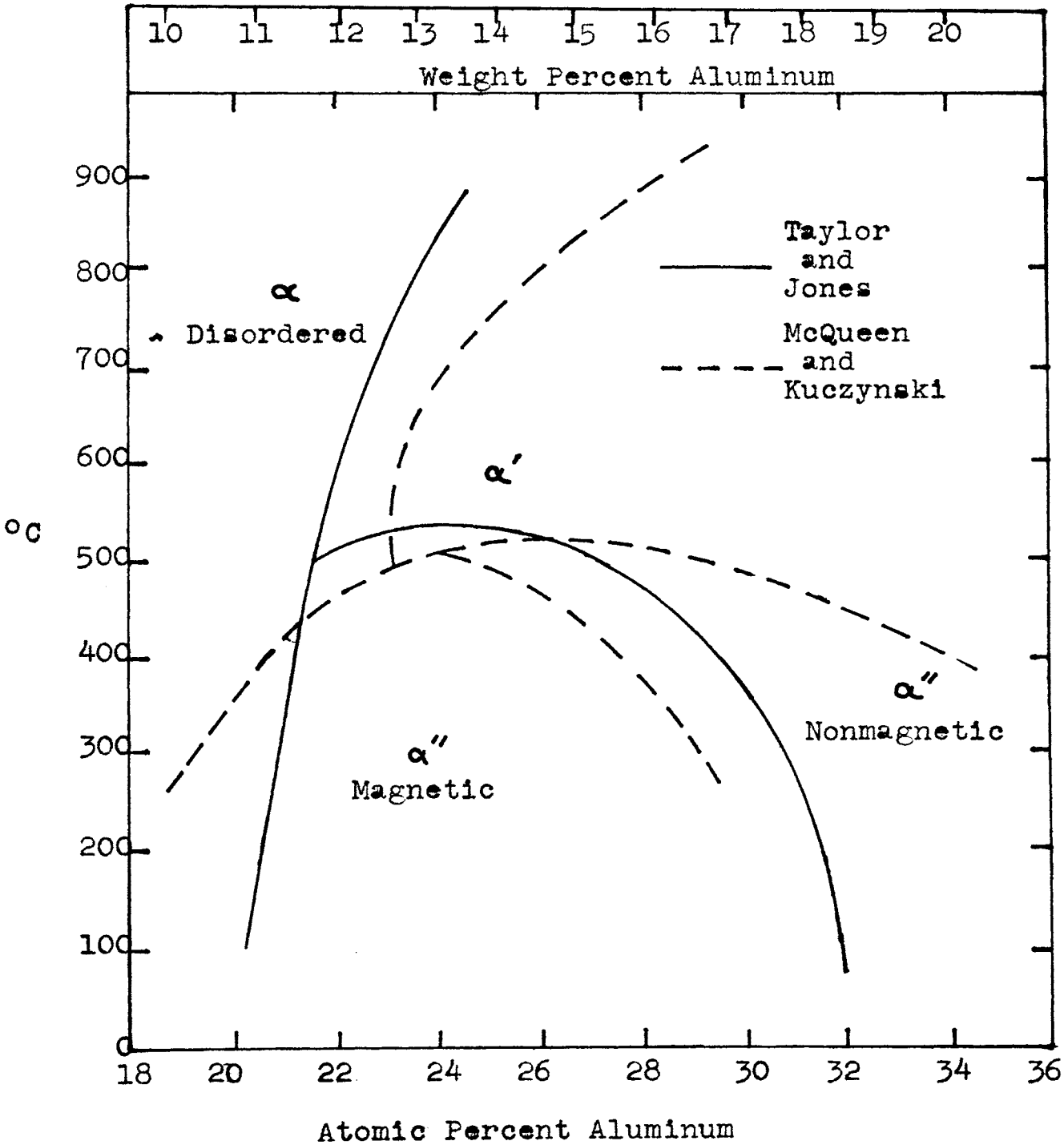

Constitution Diagram of Iron-Rich Fe-Al Alloys in the Solid Solution Range.

Figure 5.

able change in resistivity when slow cooled from high temperatures. The maximum effect, occurring at 13.9 weight percent aluminum (corresponding to the stoichiometry of Fe_3Al), represented a divergence of approximately 50 percent between resistivities of samples quenched from 700°C and those slow cooled from 700°C.

Bennet(1) studied Fe_3Al by measuring the electrical resistivity at temperatures under various rates of heating and cooling. The results of his determinations are shown in Figure 6. The evident increase in resistivity resulting from cooling the Fe_3Al from 540°C to 480°C is unexpected, since the accompanying increase in long range order would ordinarily decrease resistivity. Bennet attributes this abnormality to boundary effects between ordering nuclei.

Rauscher(23) employed resistivity measurements at elevated temperatures to determine a general outline of the atomic ordering process in Fe_3Al. The slow cooling curve of resistivity vs. temperature that Rauscher obtained, Figure 7, is similar in shape to that reported by Bennet.

NcQueen and Kuczynski(20) conducted a resistometric study of the kinetics of ordering in the Fe_3Al alloy. They calculated the equilibrium order parameter, S, for this alloy by Muto's relationship(21):

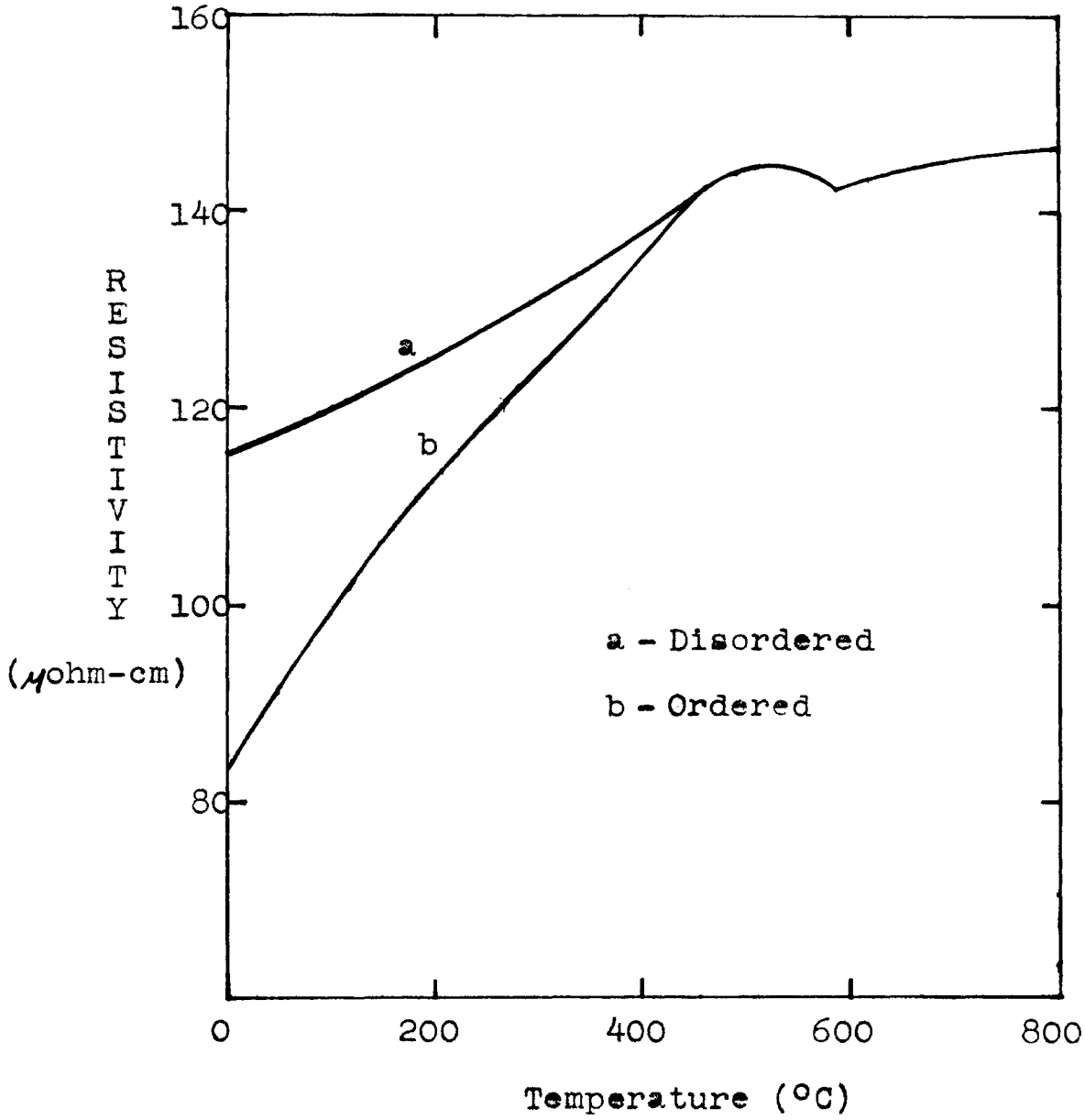

Resistivity vs. Temperature for Ordered and Disordered Fe_3Al as Determined by Bennet(1)

Figure 6.

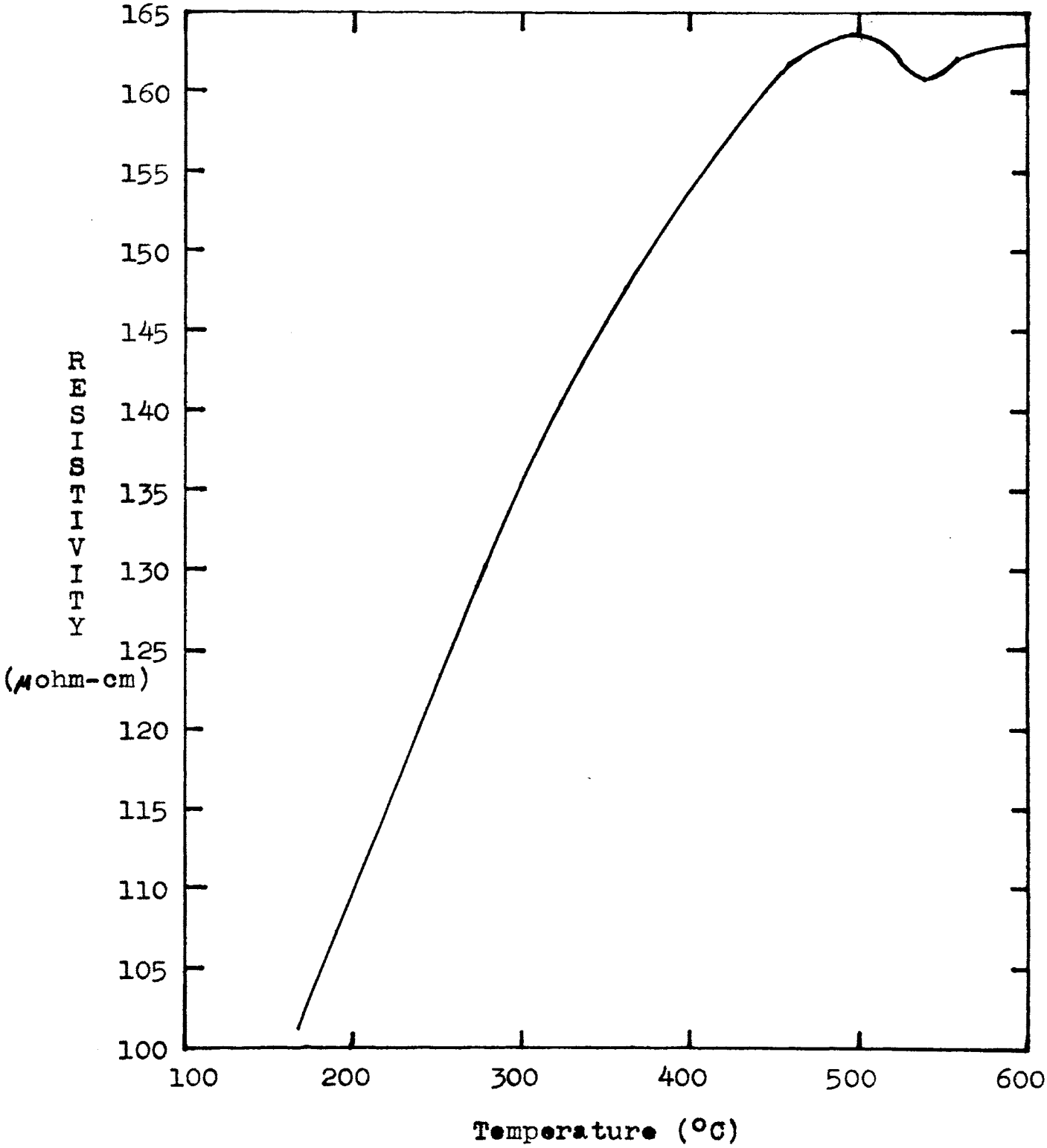

Resistivity vs. Temperature upon Slow Cooling of Fe_3Al as Determined by Rauscher(23)

Figure 7.

$$S = \sqrt{\frac{\rho_d - \rho}{\rho_d - \rho_o}} \qquad \text{(equation 2)}$$

where ρ_d is the equilibrium value of resistivity for an alloy isothermally annealed and quenched to room temperature; ρ_o is the resistivity corresponding to the order parameter S = 1; and ρ is the resistivity of the alloy equilibrated at the desired temperature and quenched to room temperature. Figure 8 is a plot of the order parameter S vs. temperature as determined by this investigation.

Leighly(16) has determined a theoretical application of the number of right atoms in "right" sites and the number of right atoms in "wrong" sites. If N is the number of atoms and S is the order parameter, then the number of Fe atoms in α sites(right) equals:

$$\frac{(3 + S)N}{8}$$

The number of Fe atoms in β sites(wrong) equals:

$$\frac{(3 - S)N}{8}$$

The number of Al atoms in α sites(wrong) equals:

$$\frac{(1 - S)N}{8}$$

The number of Al atoms in β sites(right) equals:

$$\frac{(1 + S)N}{8}$$

This can be tabulated as illustrated in Table I.

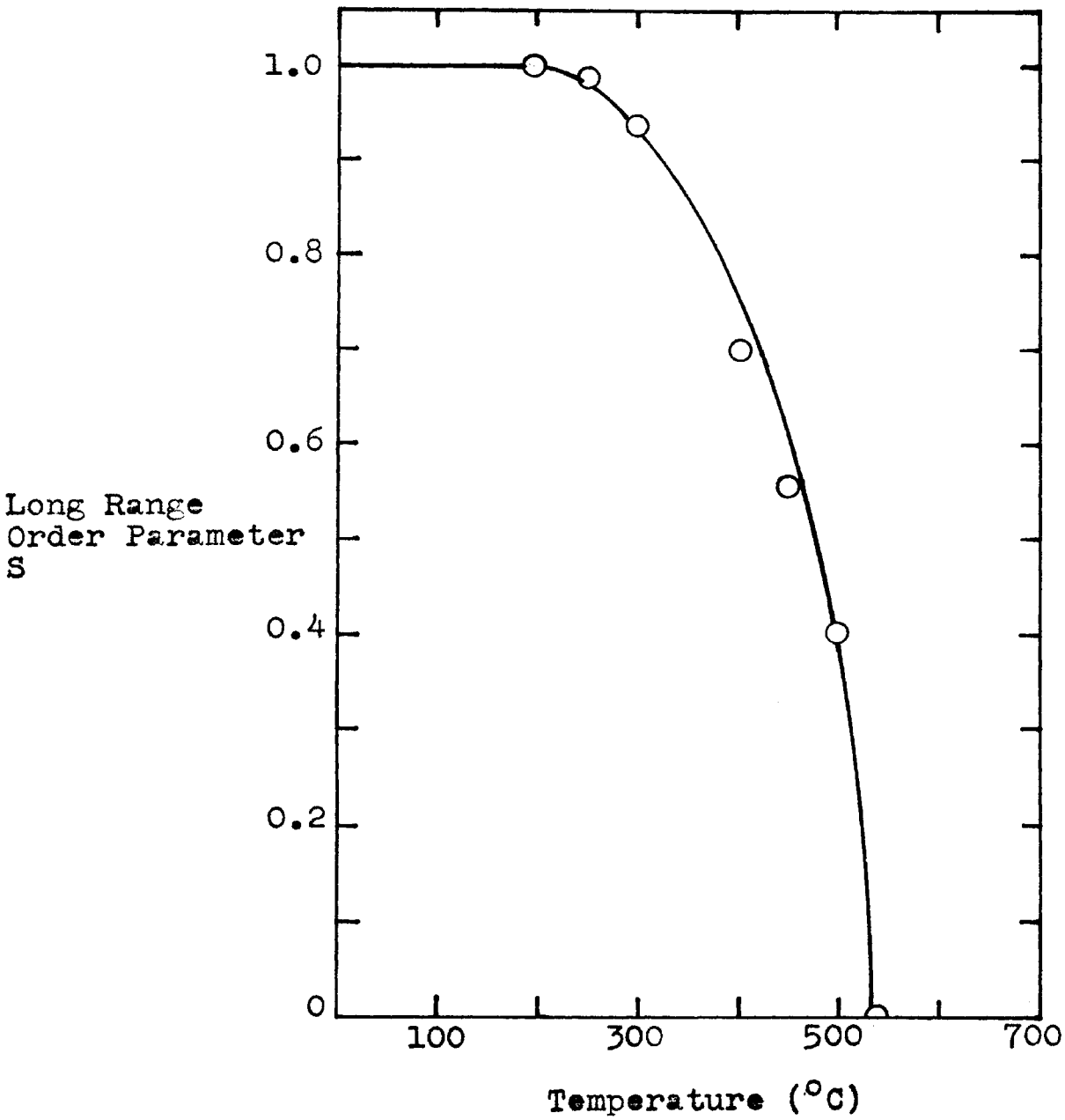

Equilibrium Degree of Fe_3Al Order as a Function of Temperature as Determined by McQueen and Kuczynski(20)

Figure 8.

TABLE I

Fe and Al in α and/or β sites

		Ordered (S=1)	Disordered (S=0)
Fe in α sites =	$\frac{(3 + S)N}{8}$	N/2	3/8N
Fe in β sites =	$\frac{(3 - S)N}{8}$	N/4	3/8N
Al in α sites =	$\frac{(1 - S)N}{8}$	0	N/8
Al in β sites =	$\frac{(1 + S)N}{8}$	N/4	N/8
	Total	N	N

He also determined the number of Fe-Fe, Al-Al, and Fe-Al bonds as follows:

$$\text{Fe-Fe bonds} = \frac{(\text{Fe in } \alpha \text{ sites})(\text{Coordination \#})(\text{Fe in } \beta \text{ sites})}{(\text{\# of } \beta \text{ sites})}$$

$$\text{Fe-Fe bonds} = \frac{\frac{(3 + S)N}{8} \times (8) \times \frac{(3 - S)N}{8}}{N/2}$$

$$\text{Fe-Fe bonds} = \frac{(9 - S^2)N}{4}$$

When S = 1, one obtains 2N Fe-Fe bonds.

When S = 0, one obtains 9/4N Fe-Fe bonds.

$$\text{Al-Al bonds} = \frac{(\text{Al in } \beta \text{ sites})(\text{Coordination \#})(\text{Al in } \alpha \text{ sites})}{(\text{\# of } \alpha \text{ sites})}$$

$$\text{Al-Al bonds} = \frac{\frac{(1 + S)N}{8} \times (8) \times \frac{1 - S)N}{8}}{N/2}$$

$$\text{Al-Al bonds} = \frac{(1 - S^2)N}{4}$$

When S = 1, one obtains N/4 Al-Al bonds.

When S = 0, one obtains 0 Al-Al bonds.

$$\text{Fe-Al bonds} = \frac{(\text{Fe in } \alpha \text{ sites})(\text{Coordination \#})(\text{Al in } \beta \text{ sites})}{(\text{\# of } \alpha \text{ sites})} + \frac{(\text{Fe in } \beta \text{ sites})(\text{Coordination \#})(\text{Al in } \alpha \text{ sites})}{(\text{\# of } \beta \text{ sites})}$$

$$\text{Fe-Al bonds} = \frac{\frac{(3 + S)N}{8} \times (8) \times \frac{(1 + S)N}{8}}{N/2} + \frac{\frac{(3 - S)N}{8} \times (8) \times \frac{(1 - S)N}{8}}{N/2}$$

$$\text{Fe-Al bonds} = \frac{(3 + S^2)N}{2}$$

When S = 1, one obtains 2N Fe-Al bonds.

When S = 0, one obtains 3/2N Fe-Al bonds.

This information is illustrated in Table II.

TABLE II

Number of Fe-Fe, Al-Al, and Fe-Al bonds

		Ordered (S=1)	Disordered (S=0)
Fe-Fe bonds =	$\frac{(9 - S^2)N}{4}$	2N	9/4N
Al-Al bonds =	$\frac{(1 - S^2)N}{4}$	0	N/4
Fe-Al bonds =	$\frac{(3 + S^2)N}{2}$	2N	3/2N
Total ➤	4N	4N	4N

Rauscher(23) utilized x-ray diffraction measurements of superlattice line intensities from single crystals of Fe_3Al to determine the relative equilibrium Fe_3Al long range order parameters as a function of temperature.

These x-ray determinations of long range order parameters indicate that the Fe_3Al disorders in a manner similar to that predicted by the Bragg-Williams theory of superlattice transformations. Rauscher found a precipitous drop from S = 0.45 at 530°C to S = 0 at 550°C.. This can be seen in Figure 9. Rauscher's diagram closely parallels McQueen's and Kunczynski's diagram. This precipitous drop, Rauscher found, infers a critical temperature near 540°C for the Fe_3Al.

The Fe_3Al superlattice, shown in Figure 4, contains 16 atoms. Of these, 12 are iron at (0 0 0), (1/2 0 0), (0 1/2 0), (0 0 1/2), (0 1/2 1/2), (1/2 0 1/2), (1/2 1/2 0), (1/2 1/2 1/2), (1/4 1/4 1/4), 1/4 3/4 3/4), (3/4 1/4 3/4), and (3/4 3/4 1/4). The four aluminum atoms are at (3/4 3/4 3/4), 3/4 1/4 1/4), (1/4 3/4 1/4), and (1/4 1/4 3/4). The superlattice reflections (ordered state) will occur for planes whose indices are either all odd or all even and whose sum is not a multiple of 4. The main lattice reflections will occur for planes whose indices are all even and whose sum is a multiple of 4 (reference 17). It should be noted here, that the main lattice reflections have Miller indices twice those occurring in α-iron because eight unit cells of body-centered cubic symmetry are required to define the Fe_3Al structure(17). The Miller indices of the main and superlattice lines of Fe_3Al are given in Table III.

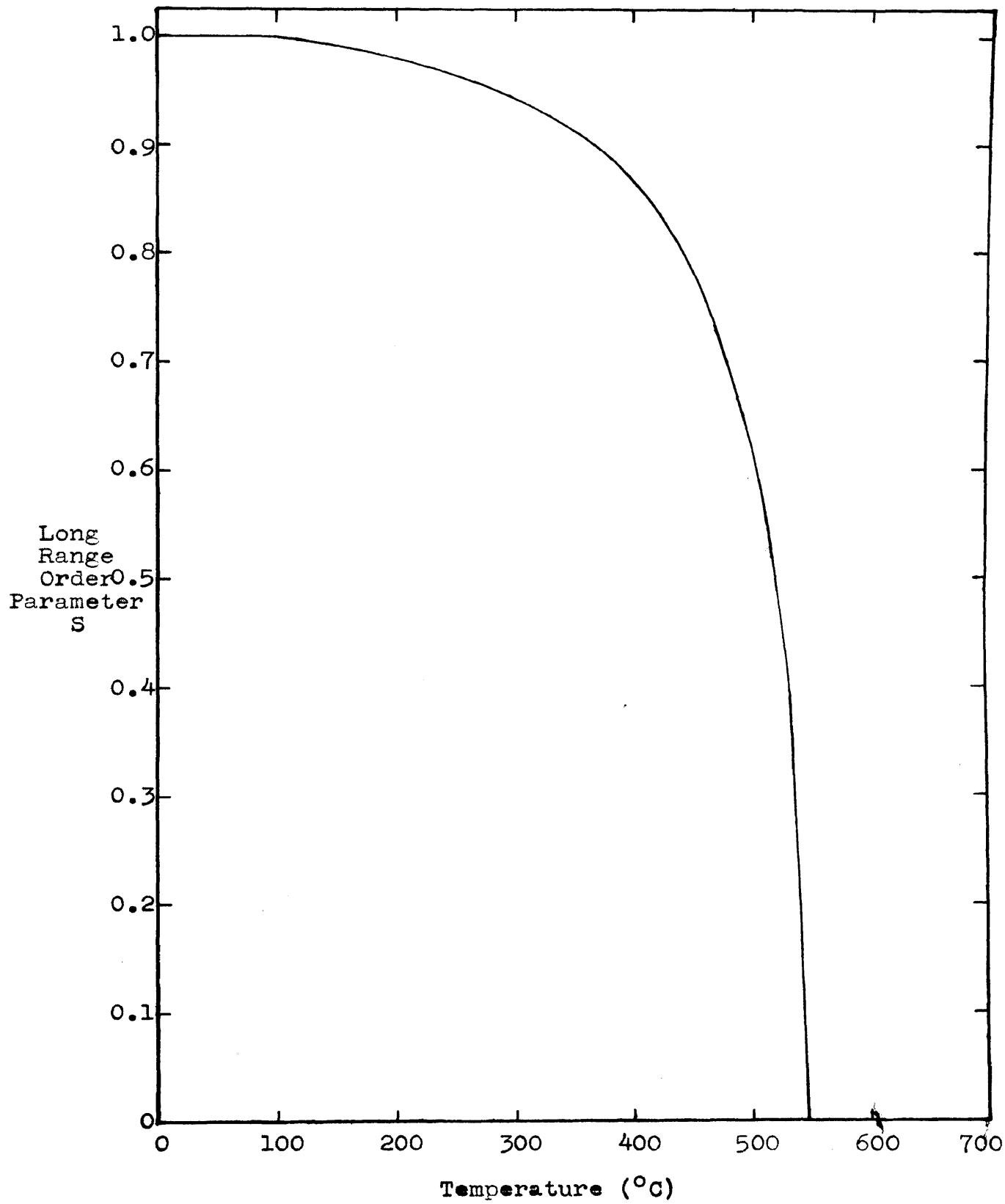

Equilibrium Degree of Fe_3Al Order as a Function of Temperature as Determined by Rauscher(23)

Figure 9.

TABLE III

Miller indices of the main and superlattice lines of Fe_3Al.

Main Lines	Superlattice Lines
220	111
400	200
422	311
440	222
	331
	420
	333
	511
	531
	442
	600

B. Effect of neutron irradiation.

The following discussion of neutron irradiation was taken in part from Dienes and Vinegard(10), Billington and Crawford(3), and Cottrell(8,9).

Everything in the core of a nuclear reactor is bombarded by neutrons, and it is these neutrons that are ultimately responsible for knocking atoms out of place and producing transmutations in the nuclei. The intensity of the neutron bombardment is measured by the "flux", the number of neutrons that pass through a surface of unit area in unit time. If, in a reactor, the neutron flux is a little greater than 10^{12} neutrons/cm^2-sec and since the cross sectional area of an atom in a solid is about 10^{-15} cm^2, each atom in the core of such a reactor has a neutron pass through it about once in 15 minutes.

A neutron is an electrically uncharged particle and so, in passing through an atom, it is unaffected by the

electrical fields centered on the nucleus and electrons of the atom. Thus, most neutrons pass straight through without the slightest disturbance to either themselves or the atom. Occasionally, however, one collides with the nucleus of the atom. Because the nucleus has a small scattering cross section, on the order of 5 barns*, the probability for such a collision is also small. This scattering cross section does not vary widely from one type of nucleus to another(30). The rate at which scattering takes place is given by the equation $R = \phi\sigma$ where σ is the cross section and ϕ is the neutron flux. This rate thus becomes equal to scatters/nuclei-sec. If a material was irradiated in a flux of 2×10^{10} neutrons/cm^2-sec and its scattering cross section is 5 barns, the rate would then be 10^{-13} scatters/nuclei-sec.

Two things can happen when a neutron strikes a nucleus. The neutron may be scattered away by the nucleus into some other direction of flight; or it may be absorbed into the nucleus itself. These are distinct processes and, in general, a given nucleus has quite different cross sections for scattering and absorption.

As stated earlier, the scattering cross section is on the order of 5 barns. Although neutrons of all speeds are scattered by nuclei, only the "fast" ones, freshly created from nuclear fission, produce radiation

* 1 barn = 10^{-24} cm^2.

damage by scattering, because only these are capable of giving a large recoil energy to the struck nucleus. The scattering of slow neutrons (i.e. moderated neutrons) forms the basis of important techniques for studying the structures of solids, but the recoil energy is too small to displace atoms.

Neutrons are usually classified in speeds according to their kinetic energies, measured in units of electron volts (1 eV is the energy acquired by an electron in falling through a potential of 1 volt). A fast neutron typically has an energy about 2 MeV, at fission, which corresponds to a speed of 2×10^9 cm/sec. A slow neutron, on the other hand, has an energy typically about 0.025 eV, which corresponds to a speed of 2×10^5 cm/sec. In this energy range, it is often referred to as a thermal neutron.

The energy given to a nucleus by a scattered neutron can be calculated from elementary mechanics. The conservation of energy and momentum limits the maximum kinetic energy E_{max} that a neutron of mass M_1 and initial energy E can give to a nucleus of mass M_2 to:

$$E_{max} = \frac{4M_1M_2E}{(M_1 + M_2)^2} \qquad \text{(equation 3)}$$

This is for a head-on collision. For collisions at other angles, the average energy transferred is $\frac{1}{2} E_{max}$. In aluminum, the value of E_{max} for a 2 MeV neutron is 0.28 MeV, while for iron, E_{max} is 0.14 MeV.

It is seen that a struck nucleus receives a kinetic

energy far in excess of the minimum value E_d (25 eV) necessary for it to jump out of its lattice site. It becomes a fast moving ion, called a primary knock-on, travelling through the material at a speed initially over 100 times faster than the speed of sound in the solid. In the face of such high energies and speeds, the lattice forces are unimportant, and the ion ploughs a track through the material in much the same way as if it vere travelling through a dense gas.

The feature that must now be taken into account is that a fast ion, created by a fast neutron collision or by a nuclear disintegration, carries a positive electrostatic charge and so interacts electrically with the electrons and nuclei that it meets on its journey. Since strong electrostatic forces are exerted between atomic particles over distances of the order of the atomic diameter, the cross section for electrostatic collisions is large and the ion is brought quickly to rest.

Because of its greater mass, an ion moves slowly compared with an electron of the same energy, and it must be examined whether a moving ion will have enough speed to excite electrons. If an electron in an atom makes a large number of oscillations during the time that the ion passes through the atom, it absorbs little energy from the ion, because the energy gained during the inward swing of an oscillation mostly is lost during outward swing.

Except at extremely high speeds, an ion will travel, not as a bare nucleus but as a charged ion with electrons in its inner atomic orbits. A rough criterion is that the ion will shake off all electrons whose speed in their atomic orbits is smaller than that of the ion itself.

Consideration must now be given to collisions between the moving ion and the lattice atoms, which can lead to the knocking of atoms out of position (secondary knock-ons). If the moving ion has sufficient energy, it can penetrate the electron cloud of an atom, so bringing the two bare nuclei face to face, unscreened by intervening electrons. The collision is then said to be of the Rutherford type, because the two nuclei interact electrostatically according to Rutherford's scattering law. But if the moving ion has insufficient energy for this, its electron cloud will not penetrate fully into that of the lattice atom, and the collision is then similar in some respect to that between hard spheres. The critical quantity is the electrostatic repulsion of the two ions at the spacing at which their nuclei are just screened by the electrons.

For primary knock-ons and for fission fragments, its energy is well above the energy E_d for producing a secondary knock-on. Thus, under these circumstances, all Rutherford collisions result in the displacement of the struck atom. The initial energy E thus becomes

shared out amongst more and more moving ions in a cascade (Figure 10).

As the average energy per ion decreases, the collisions approximate more and more closely to the hard sphere type. The two important characteristics of the latter are: 1. increased cross section so that the damage becomes very densely grouped at the end of each branch of the track, and 2. random partitioning of the kinetic energy between the striking and struck atoms. The cascade of displaced atoms thus grows by hard sphere collisions, until no atom has sufficient energy to displace another one. It is supposed that the minimum kinetic energy at which a moving atom can displace another one, without getting itself trapped in the vacancy thus created, is 2 E_d(15). Each branch of the cascade thus ends on a displaced atom with an energy of 2 E_d or less. The number of branches is thus about $E/2E_d$. If E equals $\frac{1}{2}E_{max}$ is taken, the number, n, of displaced atoms (vacancy/interstitial pairs) produced from each fast neutron collision is given by:

$$n \simeq E_{max}/4E_d \quad (15) \qquad \text{(equation 4)}$$

in materials where no energy is lost by ionization. The total concentration, c, of displaced atoms produced in a time, t, by a fast neutron flux ϕ in a material with a scattering cross section σ_s is given by:

$$c \simeq n\sigma_s\phi t \quad (15) \qquad \text{(equation 5)}$$

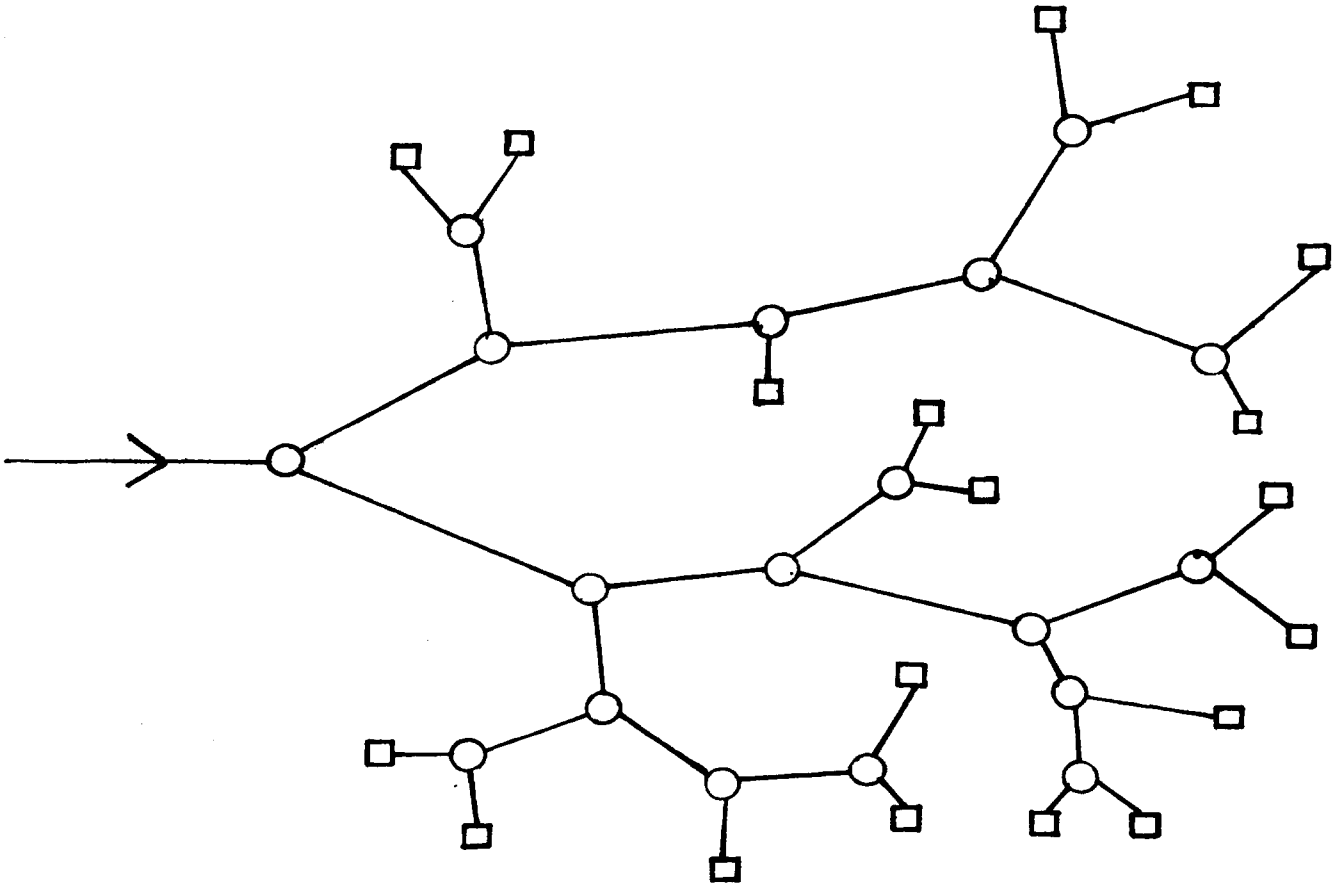

□ Interstitial Atom

○ Vacancy

A Cascade of Displacements Produced by a Fast Ion

Figure 10.

For example, if $n = 10^3$ and $\sigma_s = 4$ barns, about 4 percent of the atoms are displaced during an irradiation for 10^7 seconds in a flux of 10^{12} neutrons/cm^2-sec.

The processes that occur in the final stages of the cascade are very complex, for a large proportion of the displaced atoms undoubtedly return to lattice sites before the energy released in the cascade has dispersed. The number, n, calculated above is thus misleading to the extent that many of the displaced atoms are unlikely to survive the first few atomic vibrations of the disturbed region.

Each branch of the cascade ends at an atom that was displaced with an energy of about 2 E_d. At each collision, the displaced atom gives up about one-half of its energy to a lattice atom, which is then shared out amongst its neighbors in the form of atomic vibrations. After 10 such collisions, the atom would have an energy of less than 0.1 eV and could no longer move without receiving energy from its neighbors. It thus becomes an interstitial atom lodged within a few atomic spacings of the vacancy from which it was knocked.

The distribution of displaced atoms at the end of the track is pictured as a pear-shaped cluster containing 2n point defects spaced about 10^{-7} cm apart, with vacancies grouped preferentially toward the center, and interstitials toward the rim. If $2n = 2000$, the cluster

is about 40 atomic spacings across and contains about 60,000 atoms of which 1000 have been displaced. Since only a small part (about 5n eV) of the energy of the primary knock-on is stored in point defects, the rest of the energy must be released to atomic vibrations in the cluster. At 1 eV/atom, this is equivalent to a temperature rise (if such a macroscopic concept as heat can be used for processes on this scale) of 4000°C. The lattice forces cannot withstand such energies and, for the short period of time (10^{-12} to 10^{-20} seconds) that is necessary for the thermal pulse to disperse, the material in the cluster behaves more like a liquid than a solid. Brinkman(6) in fact, has proposed that it melts and freezes rapidly, forming a "displacement spike". During this process, the point defects in the cluster are mostly eliminated and the region freezes back on to the surrounding lattice, containing only a few quenched-in vacancies and interstitials, and perhaps a dislocation loop. If a somewhat less extreme view is taken and it is assumed that those point defects near the surface of the cluster escape annihilation in this process, then, of the n displaced atoms in the cluster, only about $n^{2/3}$ survive the displacement spike.

If a cascade of point defects can be partly annealed out by its associated thermal spike (self-annealing in the spike), then point defects may also be annealed out

by other spikes formed in the neighborhood. There is evidence for the latter in an effect known as radiation annealing(7).

Three types of annealing processes can now be distinguished. They are: 1. self-healing in the spike; 2. radiation annealing; 3. ordinary thermal annealing. Radiation annealing and thermal annealing can be separated experimentally by comparing the rates of annealing in the presence or absence of radiation. Self-healing can be recognized by the property that, in the initial stages of radiation, each spike anneals itself independently, so that the rate at which damage accumulates in the specimen is lower than is anticipated purely from collision calculations. In both radiation annealing and thermal annealing, the annealing becomes faster the more defects there are present. Thus, during an irradiation made under constant conditions, the rate at which damage accumulates should diminish with increasing doses of irradiation and eventually a saturated state should be reached in which a constant level of damage is maintained. Such effects are actually observed at large doses(15). Self-healing in the spikes thus appears to be the main reason why there are so few survivors from each collision.

The extent to which atoms change their positions from one lattice site to another is a result of irradi-

ation and is important since it may affect diffusion, phase changes, and creep in irradiated solids. There are two basically different processes by which the atoms can be redistributed: 1. by rearrangements in the thermal spike, and 2. by thermal migrations of those point defects that survive the spike. The first tends to randomize the distributions of the atoms through the lattice and can occur at all temperatures, since the energy needed to make the rearrangements is provided by the spike itself. The second occurs only at temperatures where the point defects are mobile and tends to establish the equilibrium constitution at those temperatures. Since they can act in opposite directions on the constitution of alloys, and since their relative strengths vary with the temperature of irradiation, the effects they produce can be complex. Two of these effects are order and disorder.

Good evidence for rearrangement in thermal spikes is obtained from superlattice alloys which rapidly become disordered by fast neutron irradiation at low temperatures (27) (11).

Observations on superlattice alloys have been made by Glen(13), and it has generally been supposed that the disordering is caused by rapid heating and cooling in the thermal spike.

The idea that the disordering occurs by rapid heating to a temperature where the random state is stable, fol-

lowed by the quenching-in of this random state during the rapid cooling of the spike, has been disputed. Kinchin and Pease(15) have argued that the lifetime of such a spike is too short to use the notion of temperature reliably, and they have developed instead a theory of "replacement collisions", which most of the disorder is produced by moving interstitials at the end of the cascade. These have enough energy to knock other atoms into interstitial positions, but not enough to avoid getting caught in the vacancies so created. The result is that one moving interstitial atom is replaced by another. The minimum energy needed to make such a replacement is expected to be small, perhaps about 1 eV, so that the number of replacements that can occur is large, of the order of 10^4. Seitz and Koehler(26) have expressed doubts whether the high temperatures in the spike could persist long enough to produce disordering by the heating and cooling mechanism and have argued instead that the thermal stress around a spike may be sufficient to cause plastic flow in the immediate neighborhood, and that this may be the source of disordering.

Consideration is now given to the second process whereby irradiation causes the atoms to be rearranged amongst their lattice sites -- the long range migration of point defects that survive the spikes. These migrations contribute to the diffusion coefficient of the

material and help to establish or maintain the equilibrium constitution of the material at the temperature concerned. They are important only in limited temperature range; for if it is too high, the contribution of ordinary thermally induced vacancies predominates over that of the radiation-induced defects.

Quantitative treatments have been given by Nabarro(22) and by Lomer(18). The point defects are pictured moving about randomly by thermally activated jumps from site to site, the interstitials jumping more often than the vacancies. Each defect eventually meets a site where it becomes captured or annihilated, such sites being provided by other point defects, dislocations, grain boundaries, free surfaces, and in some cases impurity atoms. The trapping occurs mainly on the type of sites in greatest abundance and hence in the earliest stages of irradiation most of the defects are annihilated or captured at boundaries, dislocations and impurity atoms. If the material is pure, and dislocations are the main sinks where the point defects are absorbed, then the number of jumps made before capture is initially of the order of 10^7, since in a typical annealed metal, one atom in 10^7 or 10^8 lies at the center of a dislocation. If, on the other hand, the material contains impurity atoms that can trap interstitials and vacancies(19), the number of jumps may be reduced to 10^4, even in rather pure (99.999%) material.

That dislocations can trap vacancies is shown by the work of Roswell and Norwick(24), who found that the rate of annealing out of point defects increases with the density of dislocations. Lomer and Cottrell(19) and Seitz and Koehler(26) have shown that some of the discrepancies between various annealing experiments on radiation damaged metals can be explained in terms of the trapping of interstitials at impurities.

The effect of neutron irradiation on the resistivity of Fe_3Al was investigated by Betts(2). He found that, at constant temperatures, the resistivity of ordered Fe_3Al would increase during irradiation and the resistivity of the disordered Fe_3Al would decrease during irradiation.

Saenko(25) also measured the resistivity as a function of fast neutron irradiation. Saenko found that the change in the electrical properties of the ordered alloy occurs as though the irradiation had disrupted the long range order existing there. He found that the ratio of the intensities of the superlattice and main reflections $I_{(111)} / I_{(220)}$ corresponded to an order parameter of $S = 0.9$ for the initially ordered alloy. When the alloy was irradiated with a flux of 3×10^{18} neutrons/cm^2, the order parameter became $S = 0.4$. After irradiation by an integrated flux of 7×10^{19} and 1.35×10^{20} neutrons/cm^2. there was complete disappearance of the superlattice lines.

In Figure 11, Saenko showed the results of the an-

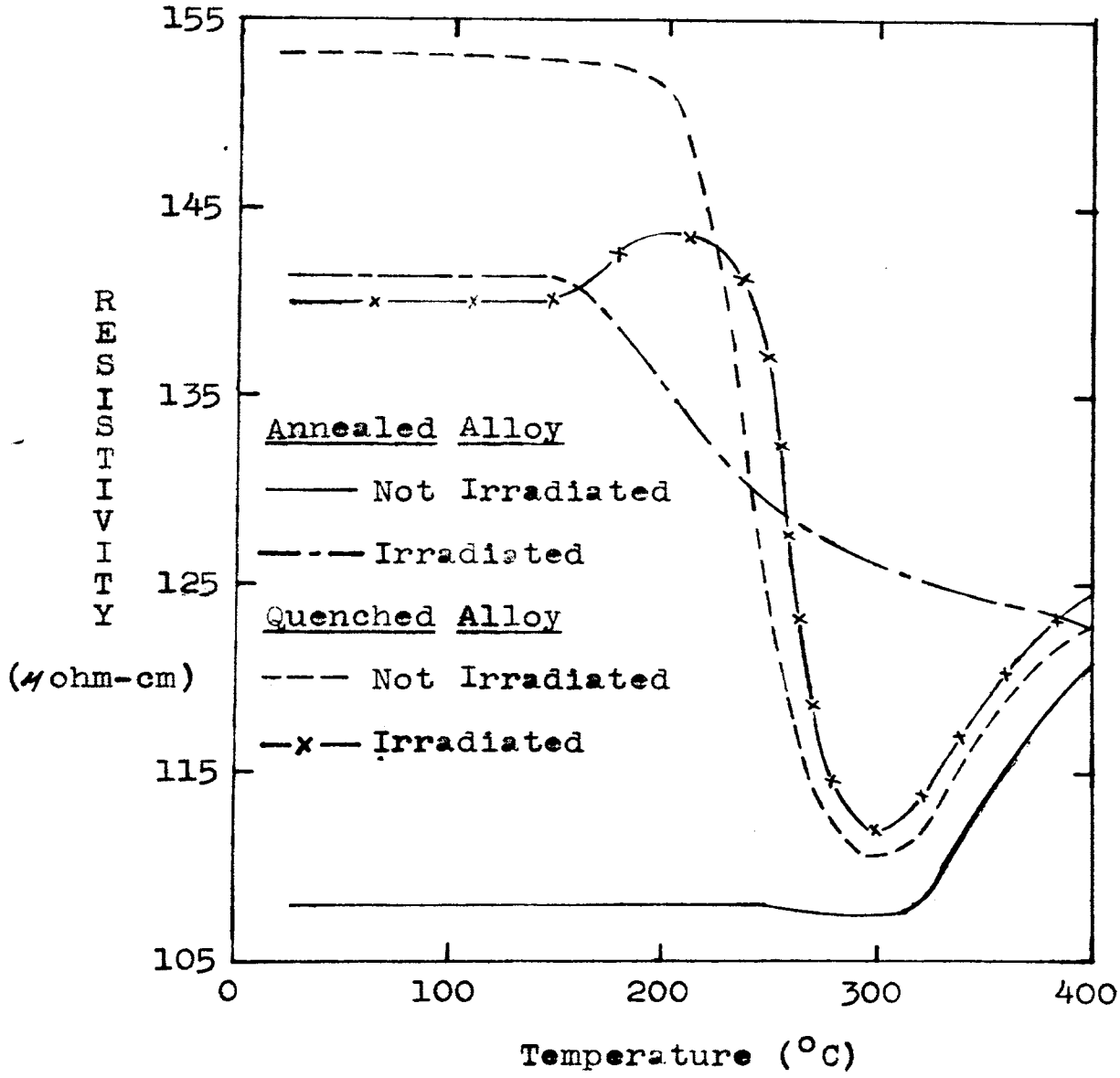

Variation of the Resistivity of Annealed and Quenched Fe_3Al, Both in the Initial State, and After Irradiation by a dose of 1.35×10^{20} n/cm^2 During the Process of isochronal Annealing.

Figure 11.

nealing of ordered and disordered samples. Both the original samples and those irradiated by a dose of 1.35 x 10^{20} neutrons/cm^2 and shown. It can be seen from the figure that the nature of the temperature change in the resistivity of the irradiated samples depends substantially on the initial state in which they were irradiated. The resistivity of the irradiated disordered alloy at first does not decrease upon heating, but increases, which is evidence of a return of part of the displaced atoms to their initial positions. It should be noted that Saenko's figure for the non-irradiated ordered alloy is completely different form Rauscher's(Figure 7) and Bennet's(Figure 6). Also Saenko's figure for the disordered sample is in complete disagreement to Bennet's (Figure 6). This tends to indicate that the rest of the data in Saenko's Figure 11 is in error.

Saenko found that the greatest change in properties is due to the disruptions that are annealed out a lower temperatures. He also found that the superlattice lines, which he said disappeared as a result of irradiation, reappeared when the ordered irradiated alloy was gradually heated to temperatures of about 200°C. This is also an indication of the return of part of the atoms displaced during irradiation to their original places. It has been shown by determining the intensity of the superlattice and main lines, that 17% of the aluminum atoms (of their total number of 25%) are arranged in their "proper"

places after the first stage of the annealing has been completed. At the same time, supplementary lines appeared when the disordered irradiated alloy was heated to 400°C.

In Figure 12, Saenko followed the path of the resistivity as a function of the integral flux. He noted that they tend toward approximately the same limit. Subsequent annealing showed that the part of the reverse change of the resistivity is quite different. This is evidence of an actual difference in the physical states arising during the irradiation process in the ordered and disordered alloys, in spite of the approximate equal values of the resistivity. The defects produced by irradiation can accelerate the process of ordering as well as do the thermal vacancies frozen in during quenching.

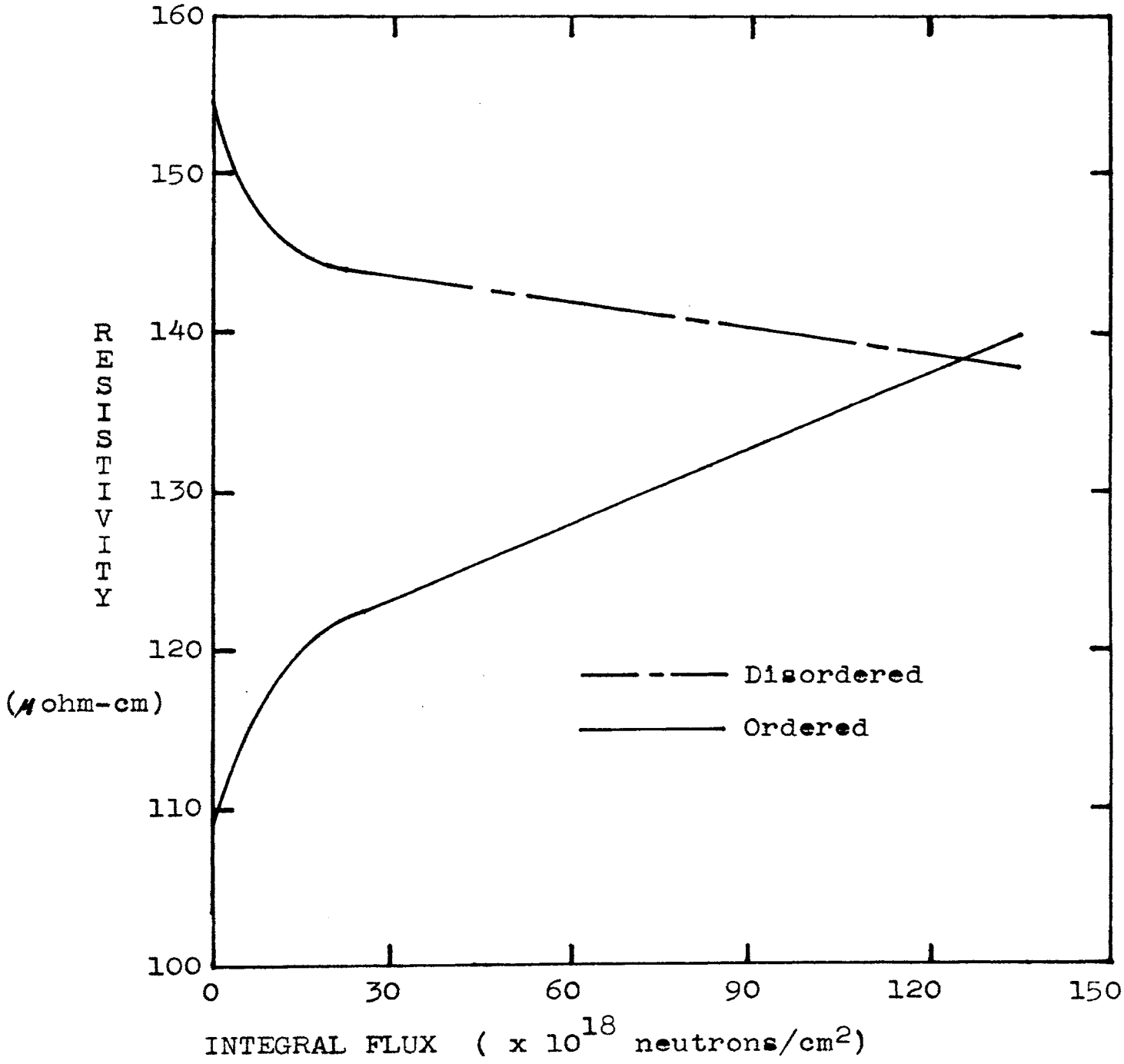

Dependence of the Resistivity of Preliminarily Ordered and Disordered Fe_3Al on the Flux as Determined by Saenko(25)

Figure 12.

CHAPTER III

EXPERIMENTAL PROCEDURE

A. Preparation of the Fe_3Al in the ordered and disordered states.

The alloy was obtained from the Naval Ordnance Laboratory in sheet form approximately 0.038 inches thick. The composition of the Fe_3Al was 25 atomic percent aluminum, 0.04% carbon, 0.03% sulfur, slight traces of silicon and phosphorus, and the remainder iron. The sheet was cut into strips approximately 0.5 inches wide by 10.75 inches long.

The ordered state was obtained by means of slow cooling of the alloy strips in the temperature interval 800 - 250°C. The strips were held at 800°C for 24 hours then cooled at a rate of 30°C per hour until a temperature of 580°C was reached. The alloy was then held at this temperature for 12 hours and was then slow cooled at a rate of 10°C per hour until it reached 500°C. The alloy was cooled at this rate for the critical temperature is in the vicinity or 540°C. After the 500°C temperature was reached, the alloy was slow cooled at 30°C per hour until a temperature of 250°C was reached. The furnace was then shut down and the alloy strips were allowed to come to room temperature.

The disordered state was obtained by means of quenching the strips from 800°C. The strips were held at 800°C for 24 hours and then quenched in a water bath.

B. Encapsulation.

When investigations in the nuclear reactor are made, materials with a low capture cross section must be used. If a material was used that did not have a low capture cross section, less neutrons would pass through the material, more will be captured, and the capsule will become too radioactive. Aluminum was picked for the capsule which would hold the Fe_3Al strip. Because the Fe_3Al strip was to be heated while inside the capsule, Al_2O_3 and SiO_2 were used as insulation. The capsule had to be water tight, so removable plugs were machined to fit both ends. The heating wire was constantan which is an alloy of copper and nickel. It was choosen for it exhibits a low capture cross section. A picture of the parts comprising the entire capsule is shown in Figure 13. A cross sectional view of the capsule is illustrated in Figure 14.

C. Temperature control.

Since the Fe_3Al strip was to be heated while it was being irradiated, the temperature had to be controlled. A Honeywell controller in line with a $7\frac{1}{2}$ amp powerstat was used. The powerstat was of sufficient amperage to heat the sample to the temperature desired.

A copper-constantan thermocouple was to be used instead of a chromel-alumel thermocouple, so the controller had to be standardized for the new thermocouple. A picture of the controller and powerstat is shown in Figure 15.

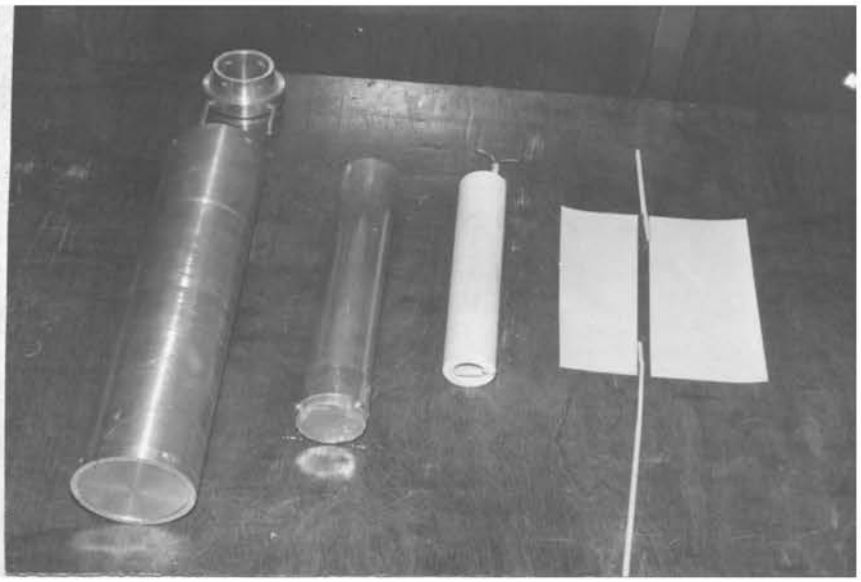

Encapsulation

Figure 13.

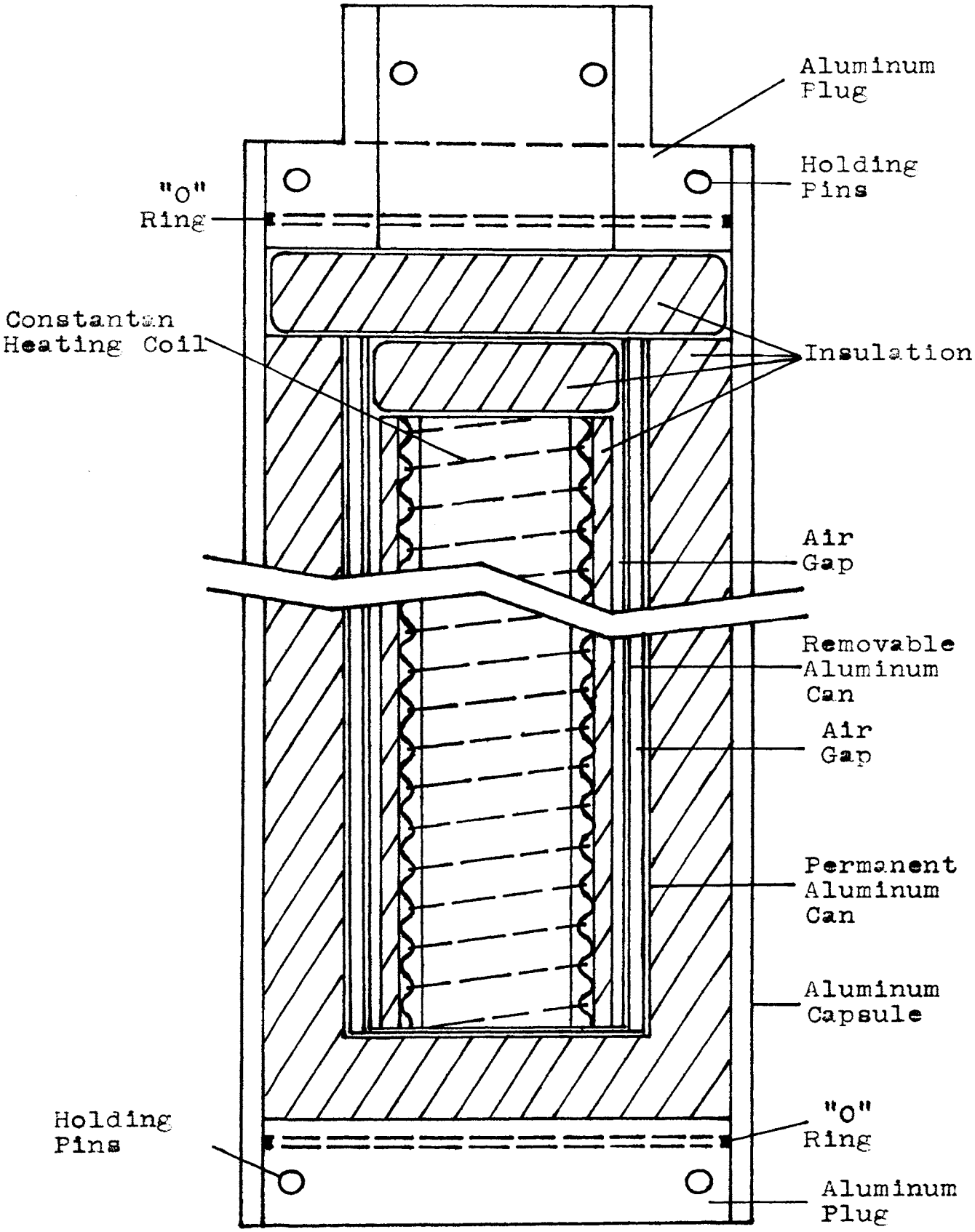

Cross sectional view of capsule

Figure 14.

Heater Controls

Figure 15.

D. Resistivity measurements.

A Kelvin double-ratio bridge resistivity apparatus with a sensitivity of 1 micro-ohm resistance was utilized in determining the resistivities as the heated Fe_3Al strip was irradiated by neutrons. Copper leads were spot welded to the ends of the samples and served as current leads to the bridge. Copper potential leads were also spot welded to the sample to provide a test length. The schematic diagram for resistivity measurements is illustrated in Figure 16.

After the leads were attached to the bridge, the heater was turned on. When the proper temperature was reached for that particular run, the bridge was then balanced. Temperatures of 100, 150, 200, 250, and 300°C were used in this investigation. Readings of resistance were then taken as the integrated fast neutron flux increased. Curves of electrical resistivity vs. fast flux were obtained for the elevated temperatures.

The resistivity, ρ, of a conductor is given by

$$\rho = \frac{RA}{L} \qquad \text{(equation 6)}$$

where R is the resistance of the conductor, A is the cross sectional area and L is the length of the test sample. The accuracy to which ρ is determined is, therefore, heavily dependent upon the accuracy to which the sample can be measured. Random readings of the

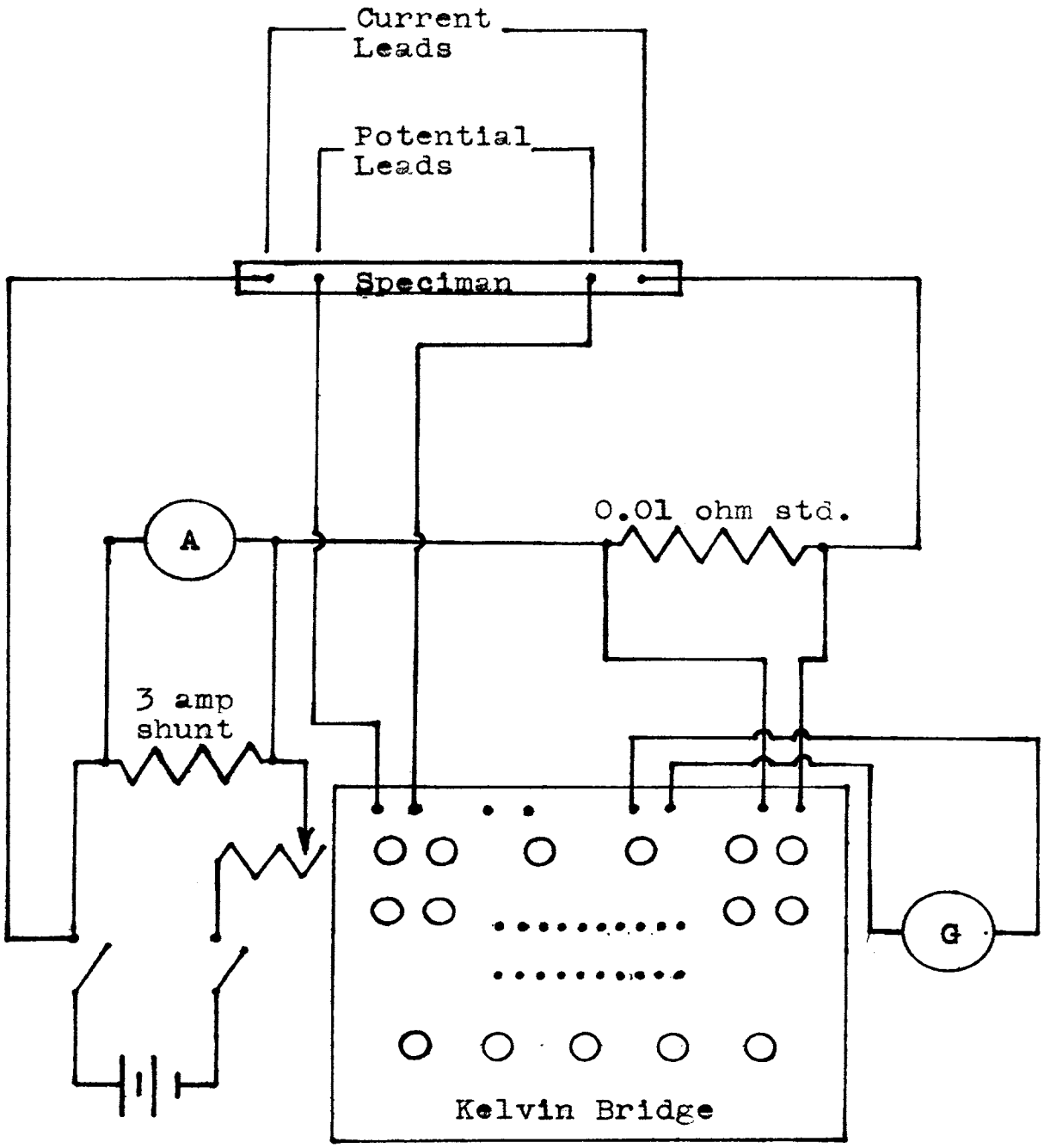

Schematic diagram for resistivity measurements

Figure 16.

sample's thickness were taken with a micrometer having graduations of 0.001 inches. Similarly, random readings of the sample's width were made. Readings were made directly to 0.001 inches. The sample's area was calculated from an average of these readings. The greatest error in calculating resistivities w s introduced in the measurements of the test length. Because the potential leads were spot welded to the sample, the distance between the leads could be measured only to an accuracy of 0.02 inches.

E. Order parameters.

After the Fe_3Al was in the ordered and disordered states, pieces of the alloy, 1½ inches long, were electrolytically polished. X-ray diffraction patterns were then made on these samples. A North American Phillips Company quadrant unit with an iron target was used.

The Fe_3Al in the ordered and disordered state exhibited uniaxial grains of about 1/32 to 1/16 inches in diameter. Because of this grain size, a spinner was used to rotate the test sample while the x-ray diffraction pattern was being produced. The test sample was rotated on the quadrant unit from 90° to 30°. A scanning speed of 1° per minute was used in conjunction with a chart speed of ½ inch per minute. After the x-ray diffraction pattern was produced, the test sample was placed in the capsule along with the test sample for

the resistivity measurements. After it was irradiated, x-ray diffraction patterns were again made on the sample.

The strip charts for both the patterns, before and after irradiation, were integrated using a polar planimeter. The integrated intensities of the (200) reflections for each sample were obtained in this manner.

The long range order parameter at a specific amount of neutron irradiation at the elevated temperature was then calculated relative to the intensity values obtained from the alloy before irradiation. If I^{o}_{200} is the integrated intensity of the (200) superlattice reflection before irradiation, and I^{x}_{200} is the intensity after irradiation, then the corresponding value of the long range order parameter, S, is calculated from:

$$S = \sqrt{\frac{I^{x}_{200}}{I^{o}_{200}}} \qquad \text{(equation 7)}$$

The Bragg-Williams treatment of superlattice transformation leads to the conclusion that perfect order (S = 1) is obtained only at absolute zero. The above method of calculating S is based on the assumption that perfect atomic order is attained at room temperature (that I^{o}_{200} corresponds to S = 1). The assumption was made to eliminate the problem of accurately correcting the errors introduced by the flat crystal geometry and other factors(21).

A long range order parameter will also be obtained

by the use of Muto's relationship (see equation 2). Since Muto's relationship requires resistivities in the calculation of the long range order parameter, the resistivities of the samples are taken at the designated test temperatures. The long range order parameter obtained by integrating the intensities are taken at room temperature after the sample has cooled. By comparing the two long range order parameters, we can see the difference that the cooling makes.

CHAPTER IV

EXPERIMENTAL RESULTS

A. Resistivity measurements.

The investigation shows that the resistivity of the Fe_3Al changes differently under the action of neutron irradiation, depending on its initial state. Thus, the resistivity of ordered(annealed) Fe_3Al, which is the least in comparison with the resistivity of the Fe_3Al in other states, increases greatly as the integrated fast flux increases. At the same time, the disordered(quenched) Fe_3Al exhibits a decrease in resistivity.

In Figure 17, a power level of 10 KW was used to determine the nature of the curve when resistivity measurements were made at 200°C for the ordered Fe_3Al. It is seen that most of the change occurs within the first two hours of irradiation at 10 KW. Therefore, it was decided to run the reactor at a power level of 2 KW for 10 hours and we would be able to determine what was happening during the early stages of damage.

In Figure 18, resistivity of ordered Fe_3Al at 100°C was measured. The initial zero reading was made at 100°C and before the neutron irradiation was started.

In Figures 19, 20, 21, and 22, the resistivities were measured at temperatures of 150, 200, 250, and 300°C, respectively, and at a power level of 2 KW. As was seen in the resistivity measurements at 10 KW, the greatest

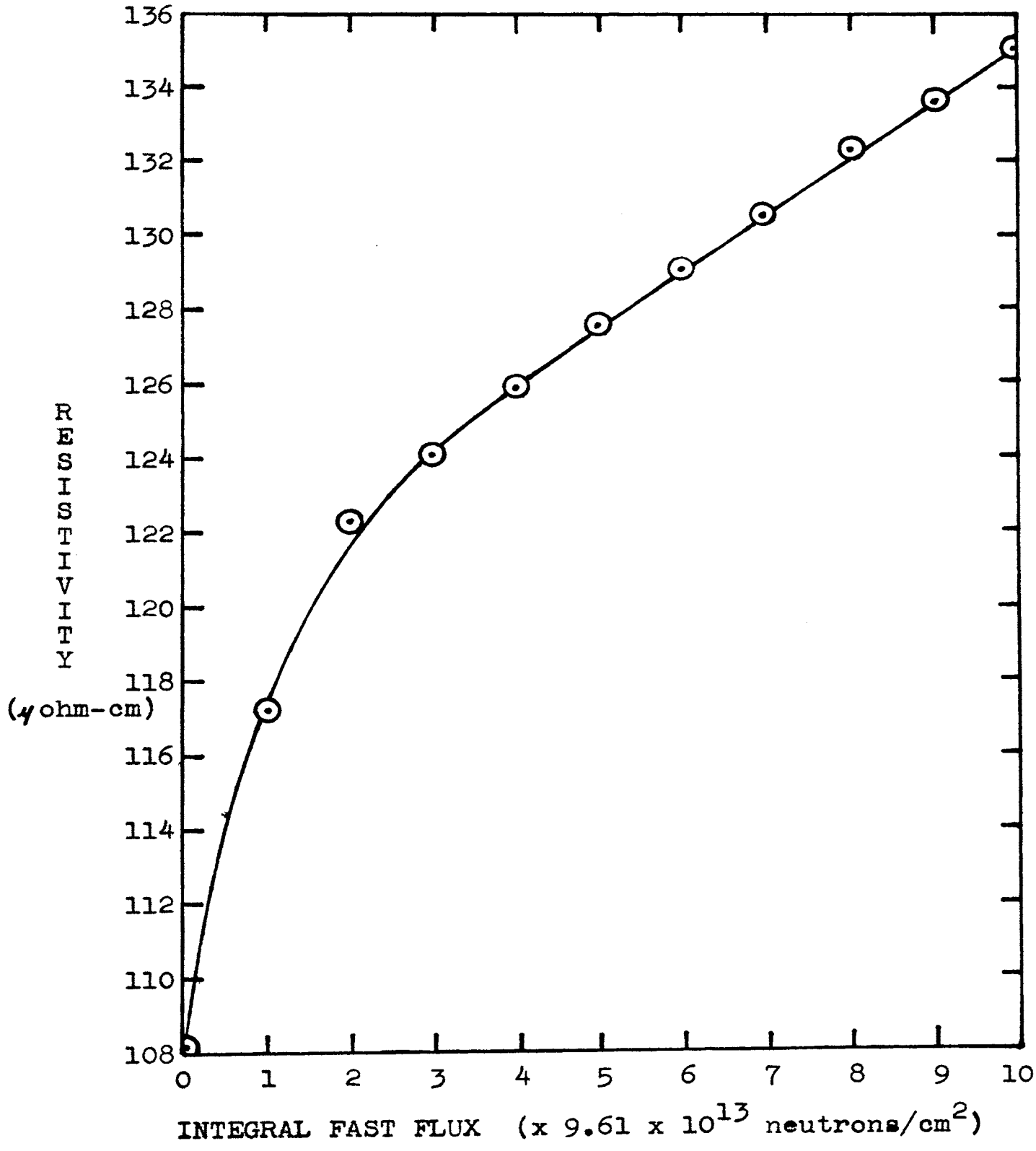

Resistivity vs. flux (Fe_3Al at 200°C)

Figure 17.

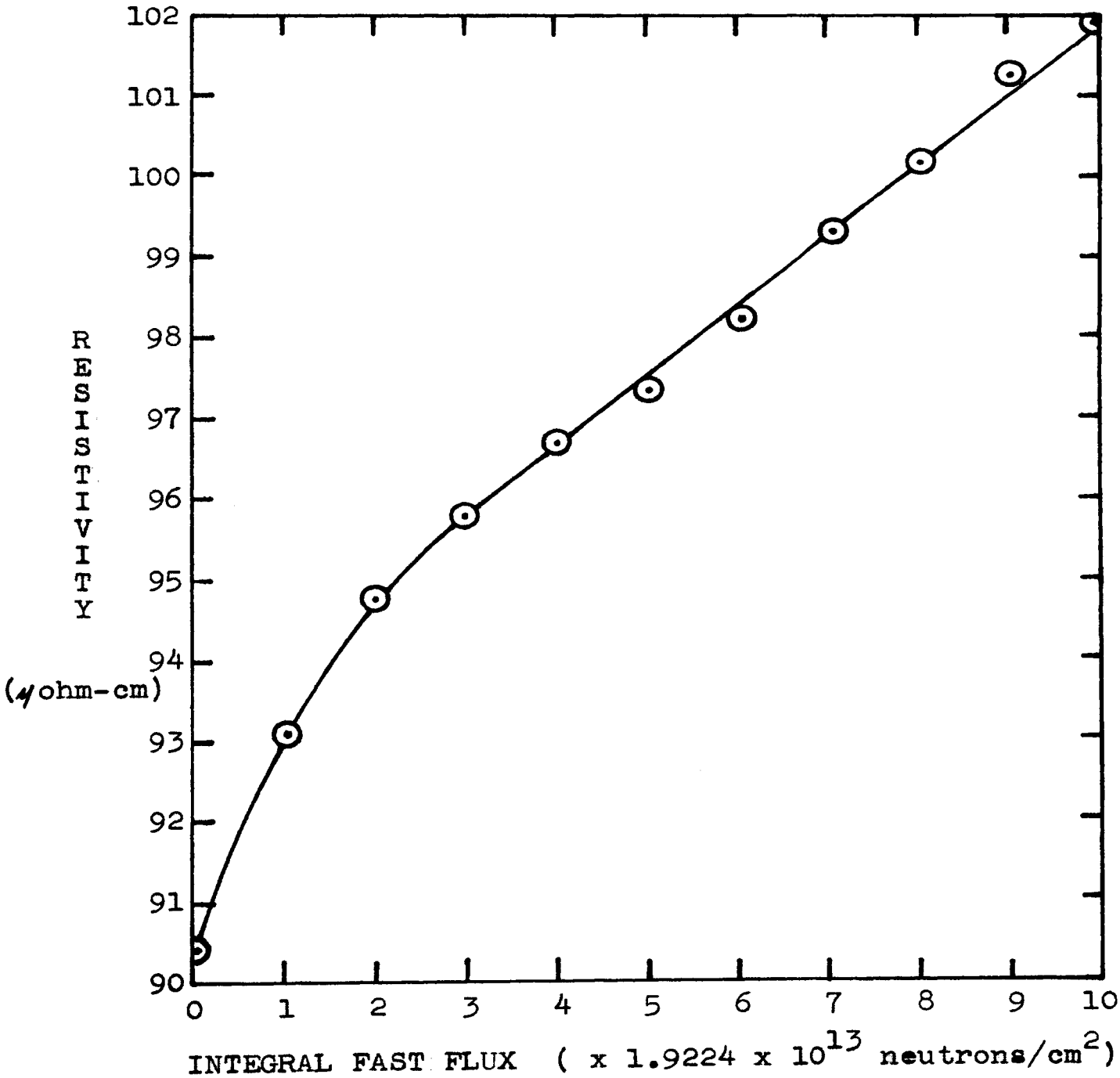

Resistivity vs. Flux (Fe_3Al at 100°C)

Figure 18.

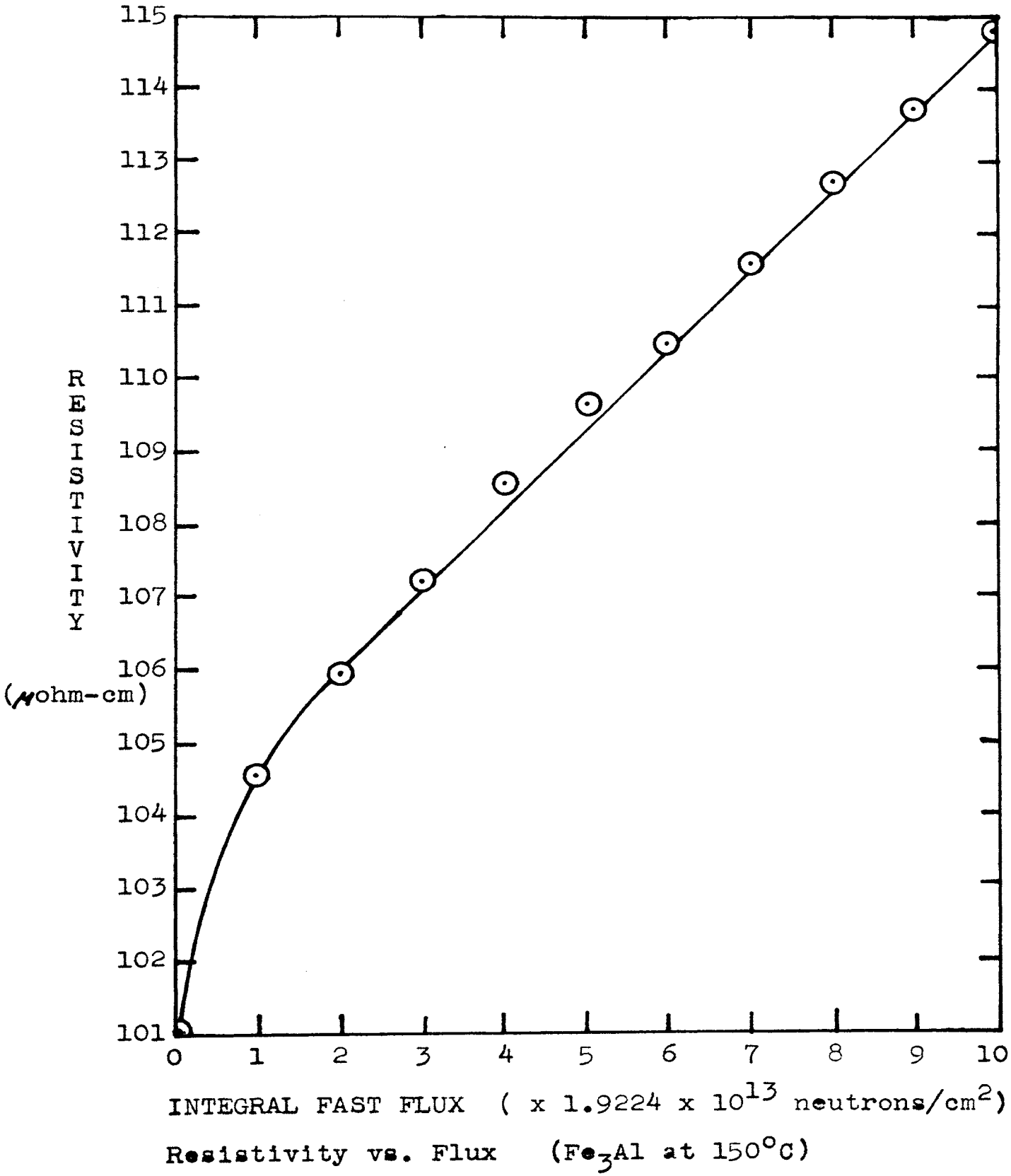

Resistivity vs. Flux (Fe_3Al at 150°C)

Figure 19.

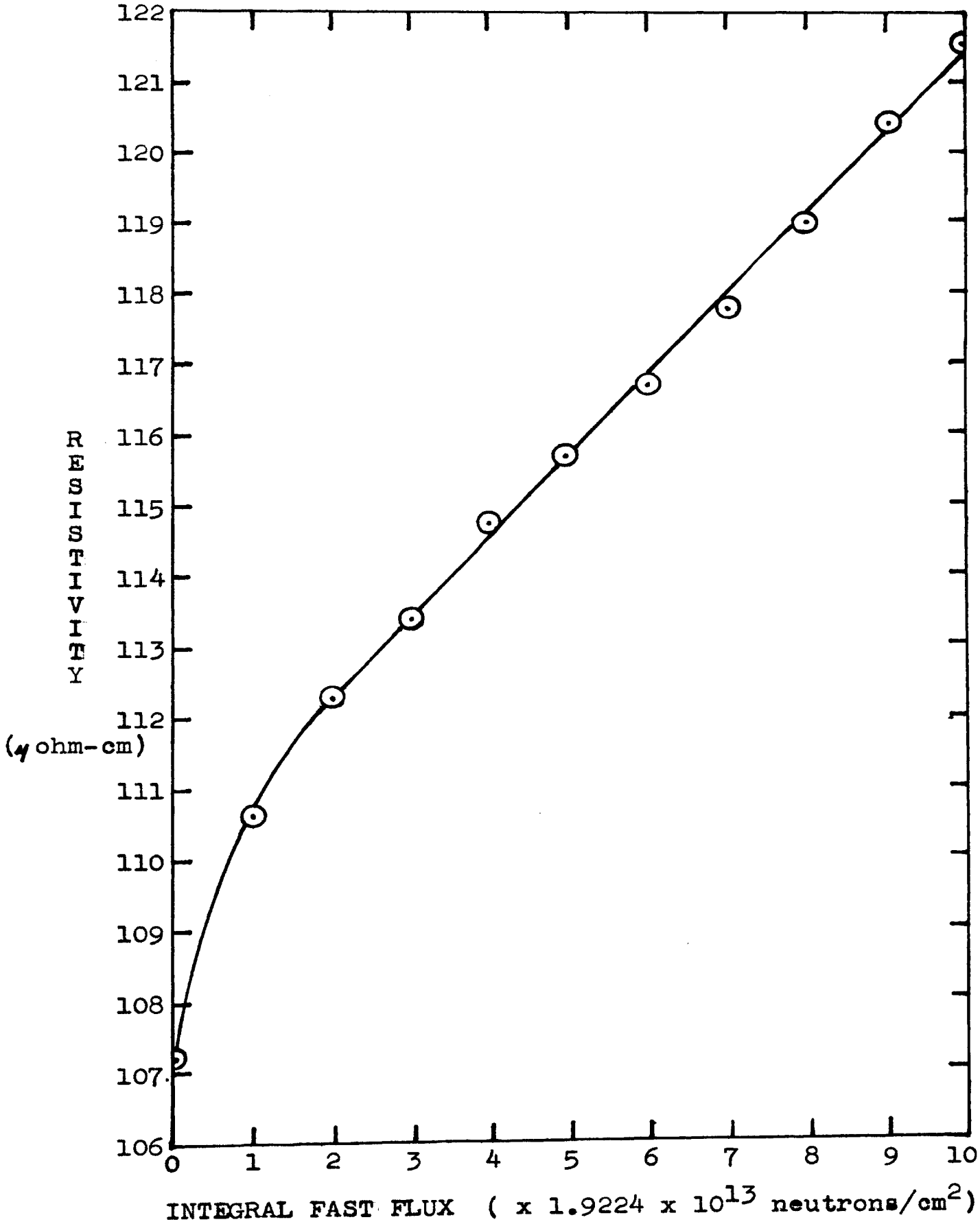

Resistivity vs. Flux (Fe_3Al at 200°C)

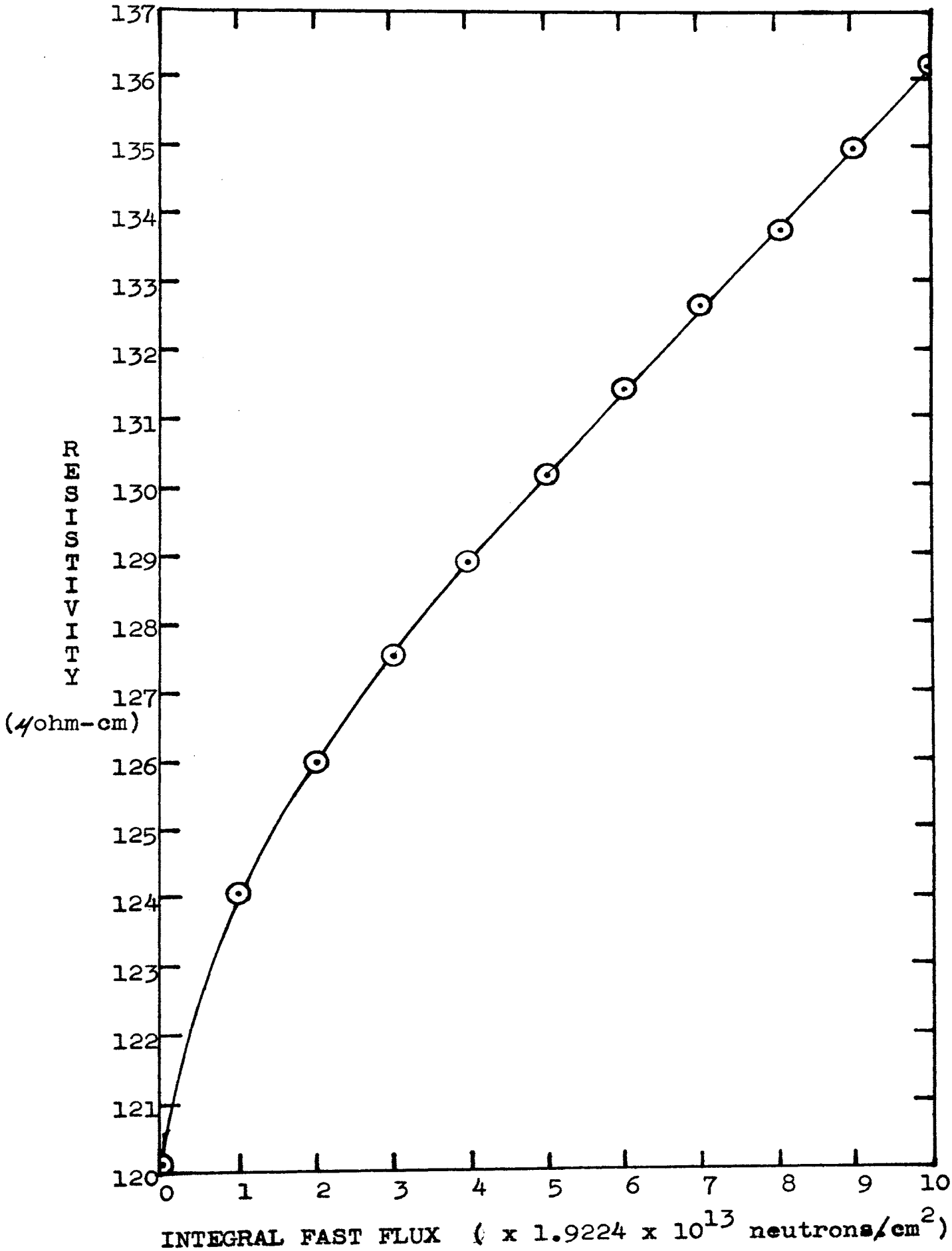

Resistivity vs. Flux (Fe_3Al at 250°C)

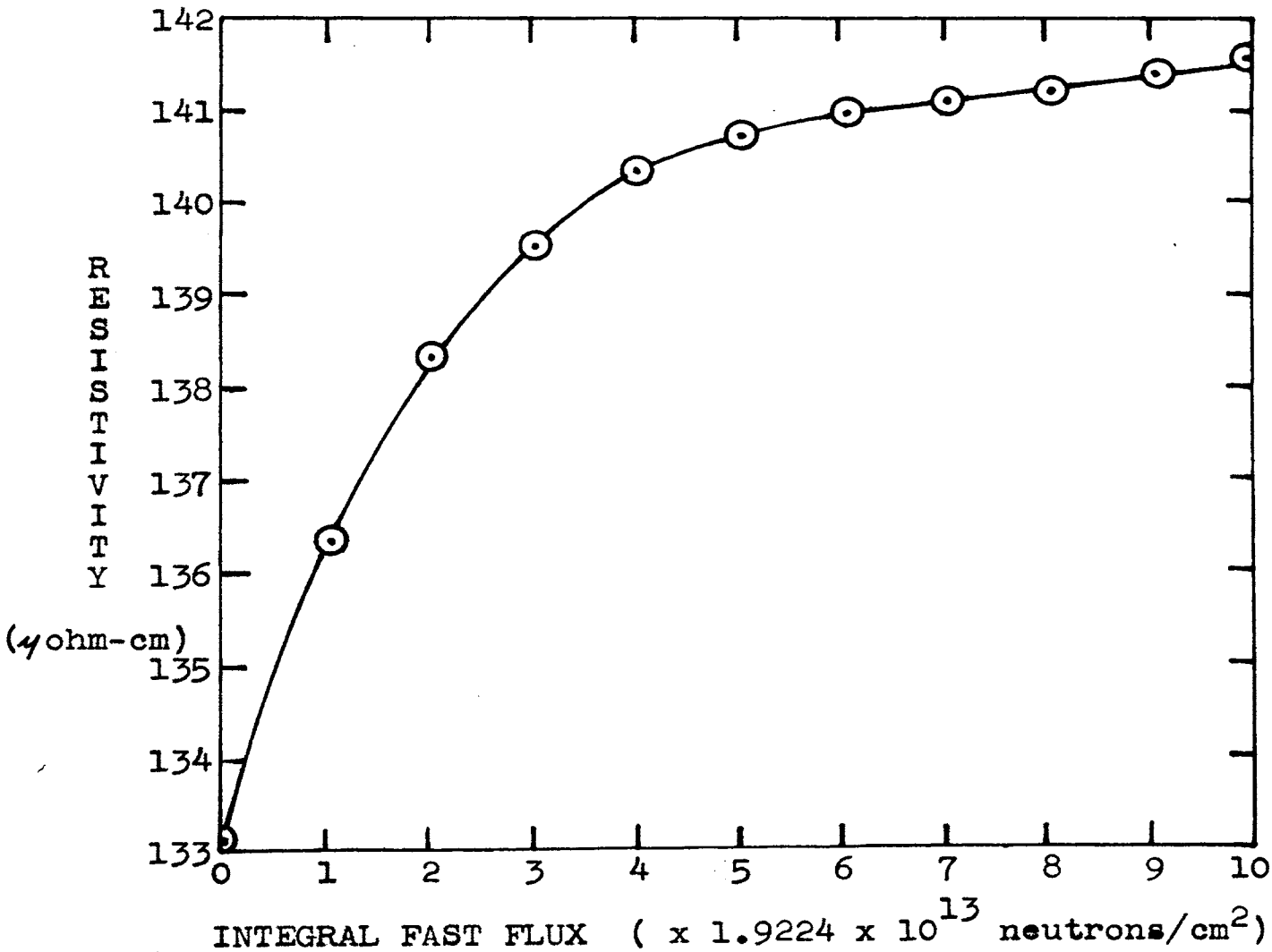

Resistivity vs. Flux (Fe_3Al at 300°C)

Figure 22.

change also appeared during the initial irradiation at 2 KW. The initial resistivity measurements(at zero flux) correspond to the resistivity of the Fe_3Al at the elevated temperatures.

In Figure 22, where the resistivity vs. integral fast flux was measured at 300°C, the curve begins to approach a constant resistivity.

In Figures 23, 24, 25, 26, and 27, the resistivity vs. integral fast flux for the disordered Fe_3Al was measured at temperatures of 100, 150, 200, 250, and 300°C respectively. Since the samples were quenched from the same temperature, the initial resistivities are approximately the same. It should be noted that after an irradiation of 19.2×10^{13} neutrons/cm^2, the curves arrived at the same approximate resistivity of 142 μohm-cm. As the temperature increases, the rate of ordering increases and the higher the temperature, the more the curve tends toward a constant resistivity.

If the curve for the ordered Fe_3Al at 300°C (Figure 22) and the curve for the disordered Fe_3Al at 300°C (Figure 27) are taken, it is seen that they both tend toward approximately the same limit.

If the samples for both the ordered and disordered Fe_3Al at the same temperatures, had been irradiated more, they should also tend toward the same limit.

B. Order parameter.

One of the order parameter vs. temperature curves

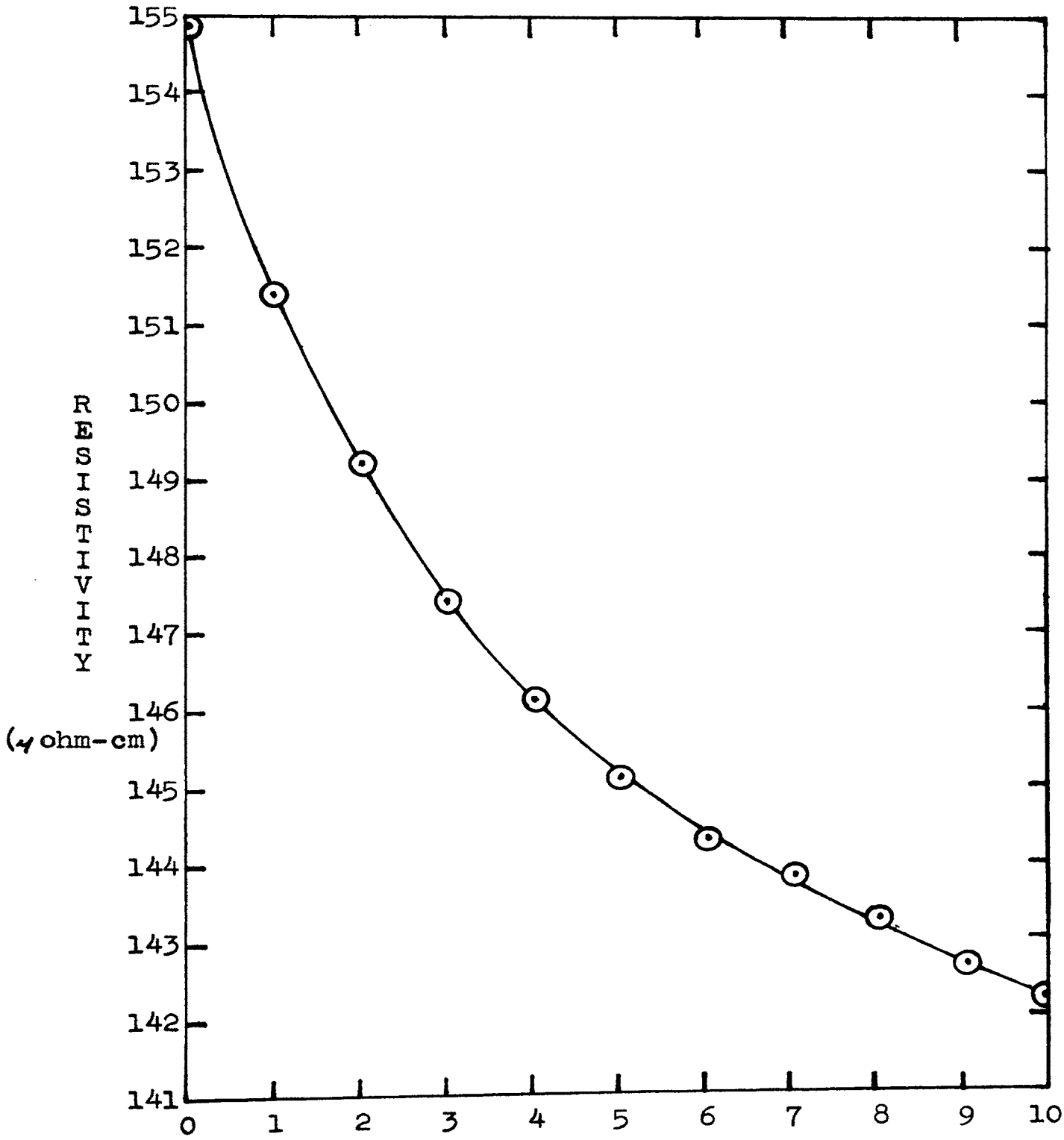

Resistivity vs. Flux (Fe_3Al at 100°C)

Figure 23.

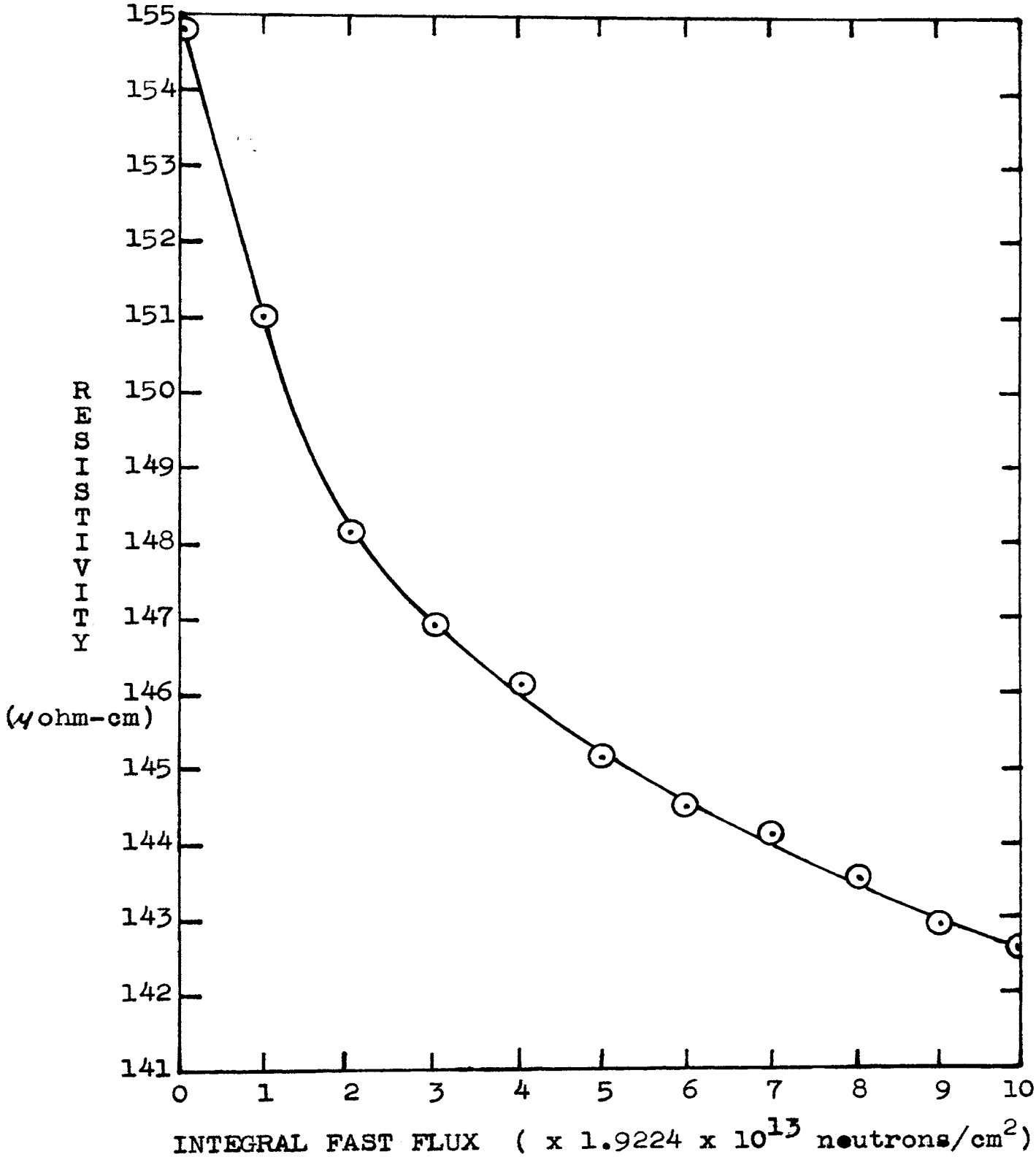

Resistivity vs. Flux (Fe_3Al at 150°C)

Figure 24.

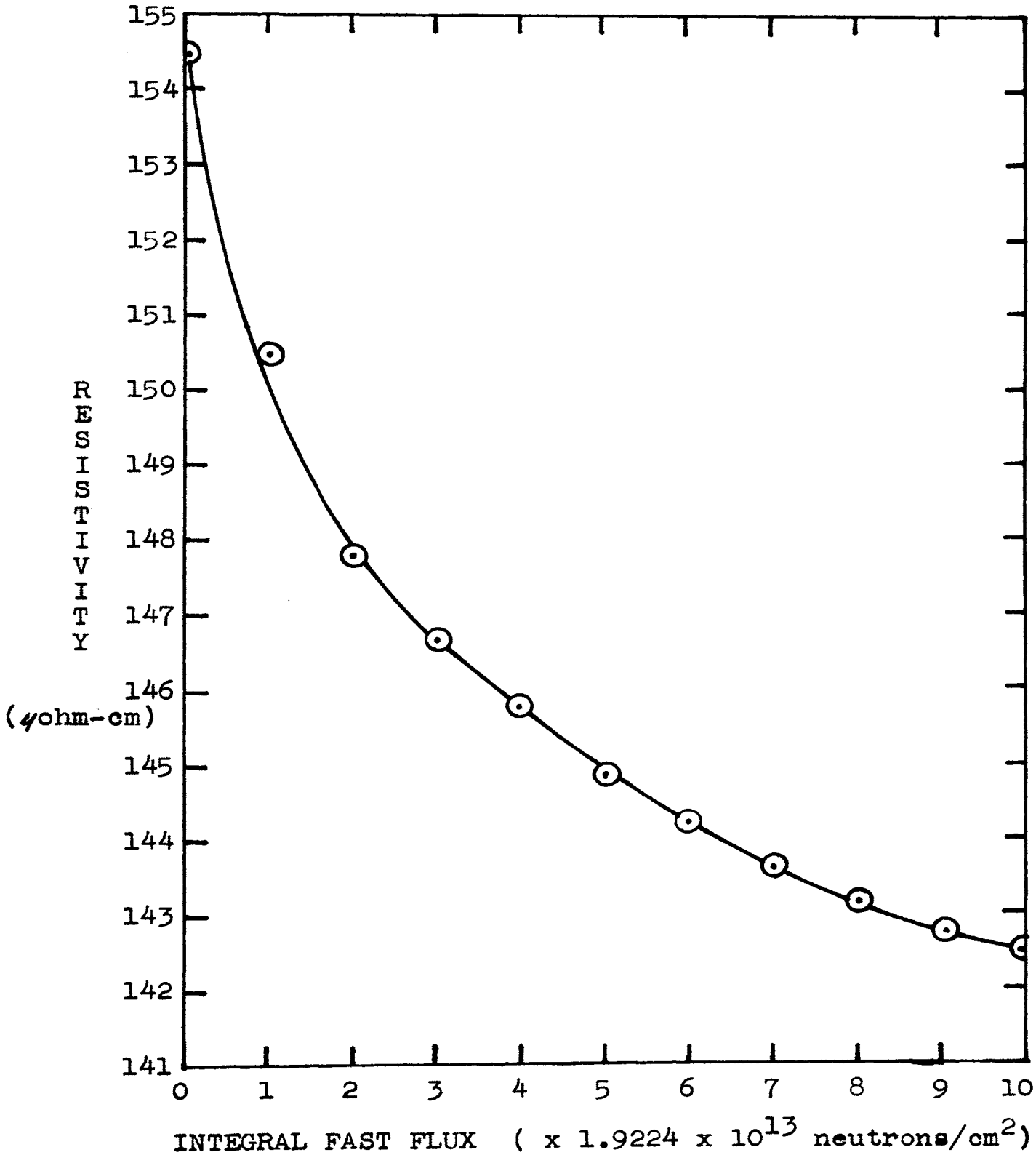

Resistivity vs. Flux (Fe_3Al at 200°C)

Figure 25.

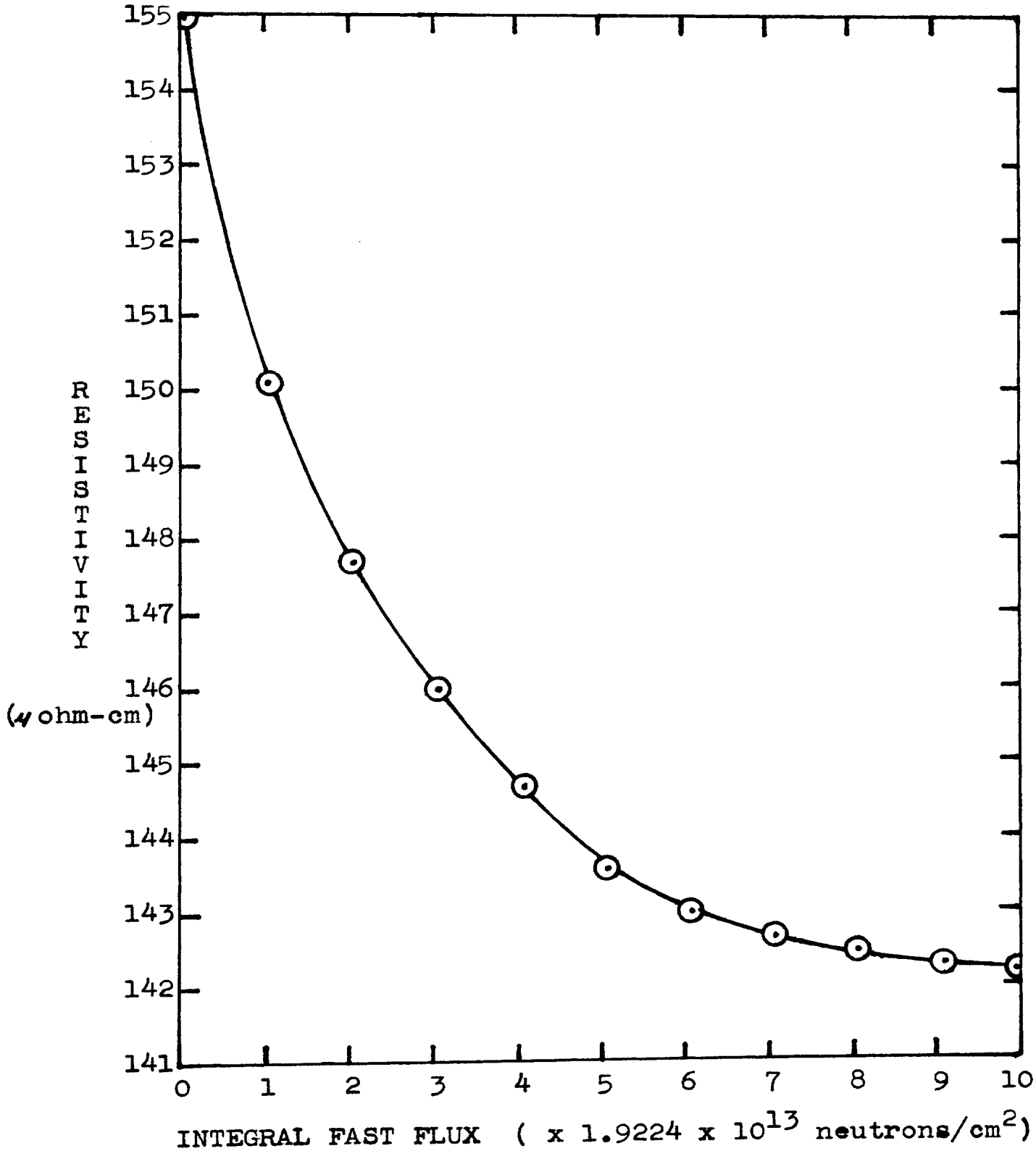

Resistivity vs. Flux (Fe_3Al at 250°C)

Figure 26.

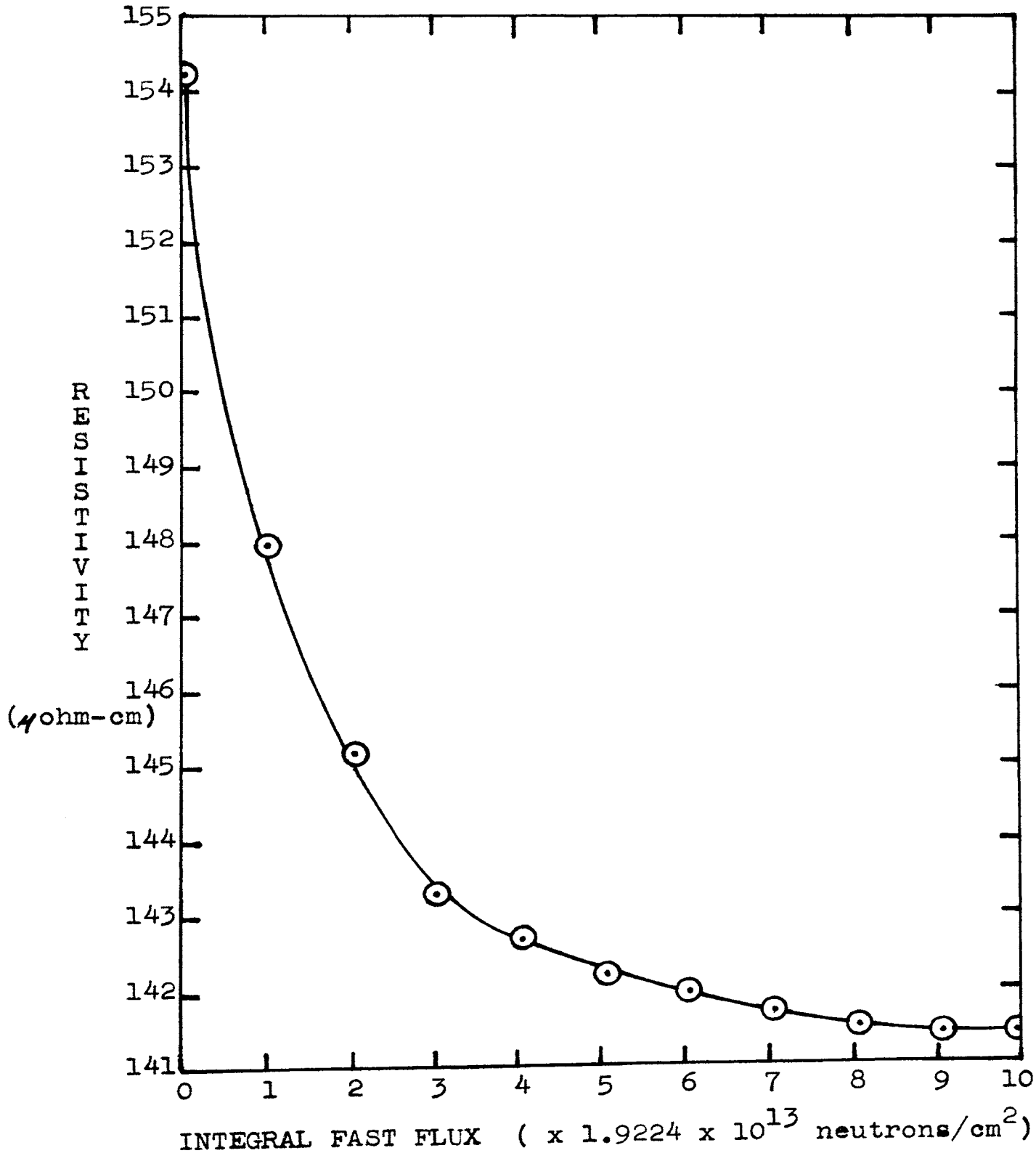

Resistivity vs. Flux - (Fe_3Al at 300°C)

Figure 27.

for initially ordered Fe_3Al, illustrated in Figure 28 was obtained by Muto's relationship (see equation 2). ρ_d was taken as the average resistivity of the five initially disordered Fe_3Al samples at zero flux and is equal to 154.7 μohm-cm. ρ_o was taken as the initial resistivity of the ordered sample at 100°C and zero flux and is equal to 90.4 μohm-cm. ρ is now the resistivity of the Fe_3Al sample irradiated by a dose of 19.2×10^{13} neutrons/cm^2 at 100, 150, 200, 250, and 300°C.

The other curve in Figure 28 was obtained by the integrated intensity of (200). I^o_{200}, which corresponds to an order parameter of S = 1, was approximately the same for the five initially ordered Fe_3Al samples that were irradiated at 2KW and is equal to 210 mm^2. I^x_{200}, which is the integrated intensity after irradiation by a dose of 19.2×10^{13} neutrons/cm^2, has values of 150 mm^2 for the sample irradiated at 100°C, 165 mm^2 for the sample irradiated at 150°C, 170 mm^2 for the sample irradiated at 200°C, 190 mm^2 for the sample irradiated at 250°C, and 190 mm^2 for the sample irradiated at 300°C.

If Muto's relationship is used to determine the order parameter for the initially disordered Fe_3Al, a straight, almost horizontal, line is obtained (Figure 29). This happens because the resistivities of the disordered Fe_3Al samples, after an irradiation of 19.2×10^{13} neutrons/cm^2, are approximately constant.

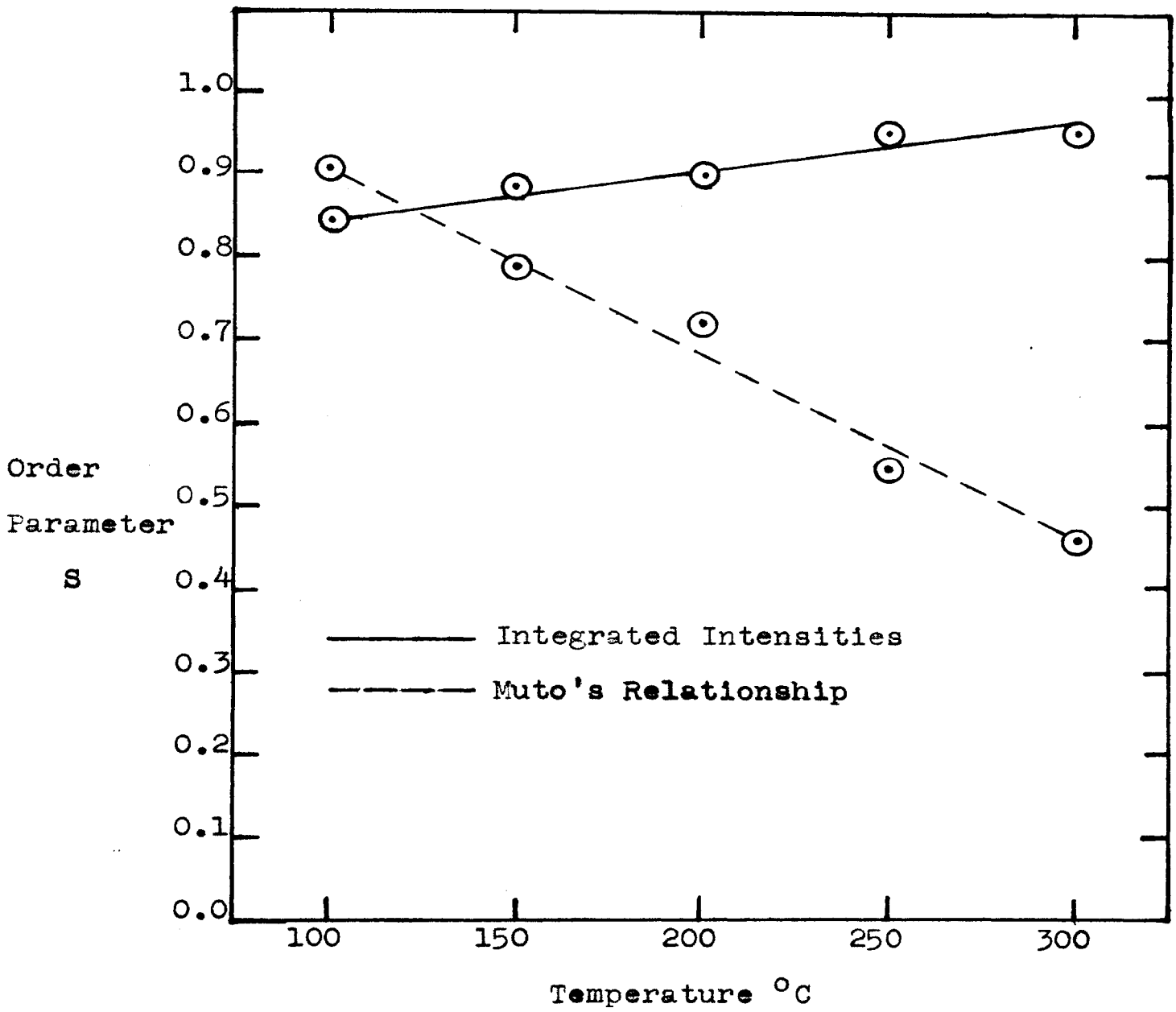

Initially Ordered Fe_3Al Order as a Function of Temperature and Fast Neutron Flux.

Figure 28.

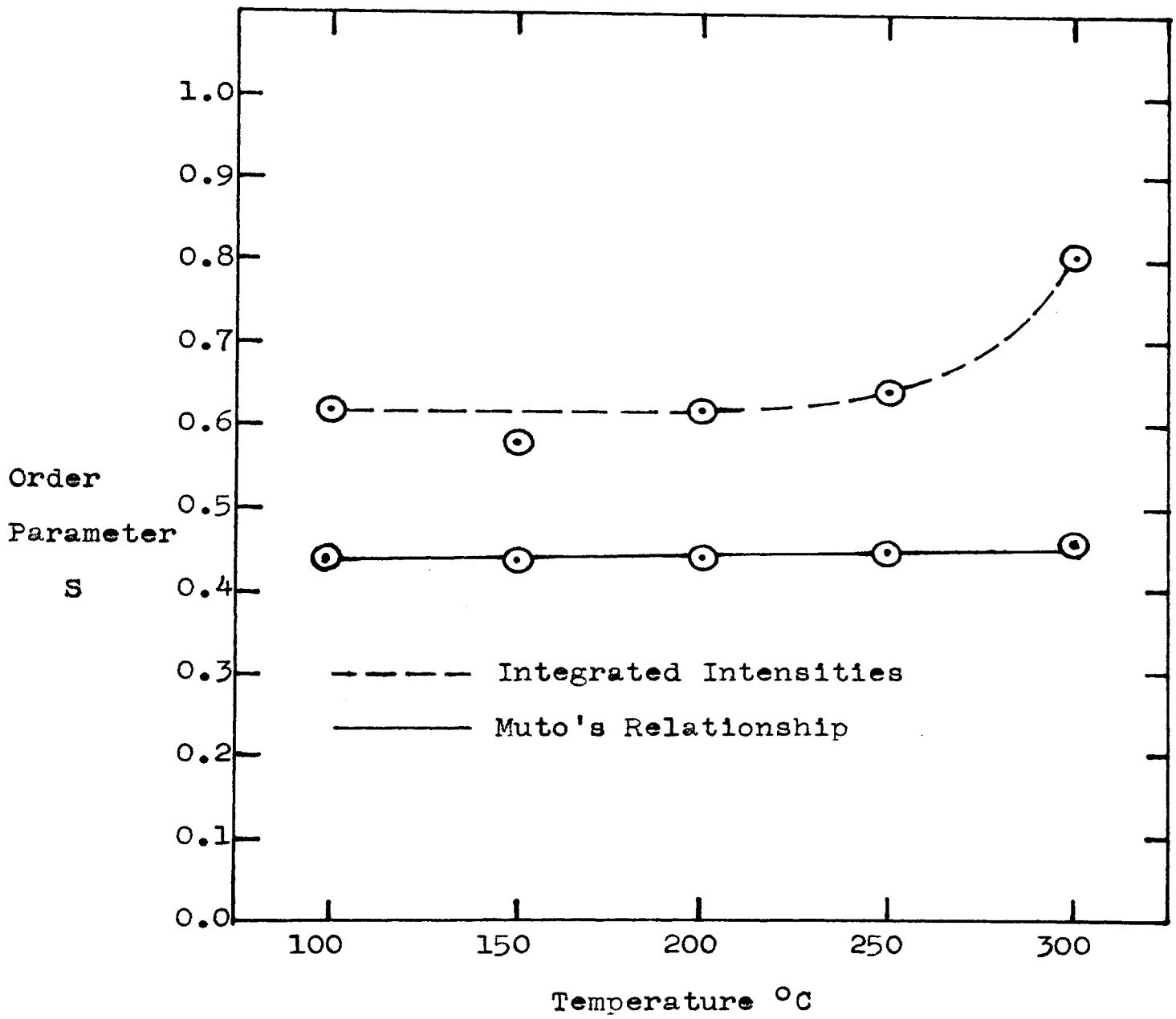

Initially Disordered Fe_3Al Order as a Function of Temperature and Fast Neutron Flux.

Figure 29.

For initially disordered Fe_3Al, the order parameter obtained by use of the integrated intensities is also illustrated in Figure 29. Again the value of I^o_{200} was taken as 210 mm^2. The values of I^x_{200} are 80 mm^2 for the sample irradiated at 100°C, 70 mm^2, for the sample irradiated at 150°C, 80 mm^2 for the sample irradiated at 200°C, 85 mm^2 for the sample irradiated at 250°C, and 135 mm^2 for the sample irradiated at 300°C.

CHAPTER V

DISCUSSION OF RESULTS

This investigation on Fe_3Al was the first one carried out at elevated temperatures during neutron irradiation. Other experiments, Betts(2) and Saenko(25), were carried out at ambient temperatures. It is, therefore, difficult to compare the results obtained in this investigation with the other investigations.

It can be stated, though, that this investigation showed that the ordered Fe_3Al became more disordered when irradiated by neutrons and that the disordered Fe_3Al became more ordered when neutron irradiated. Also, the resistivities of the ordered and disordered Fe_3Al at the same temperature, tend to become constant, indicating that the amount of ordering and disordering reached equilibrium. This equilibrium is approximately one-half the way between the initial resistivities (before irradiation) of the ordered and disordered Fe_3Al. This was quite apparent in the investigation at 300°C, for the resistivities of both the initially ordered and disordered Fe_3Al became constant at approximately the same resistivity which was one-half the way between the initial resistivity measurements.

The resistivities of the initially disordered Fe_3Al, upon irradiation of 19.2×10^{13} neutrons/cm^2, all tended toward the same value of 142 μohm-cm. The only

difference in the curves obtained for the irradiation of disordered Fe_3Al at various temperatures was in the initial rate of ordering. The higher the test temperature, the faster the initial rate of ordering.

For disordering to take place, the mechanism is attributed to the formation of vacancies and interstitials which are sufficiently mobile to allow necessary micro-diffusion. The vacancy/interstitial pair generated is called a Frenkel defect. Other metals that do not exhibit an order-disorder transformation as does Fe_3Al, have their resistivities increase much more slowly than ordered Fe_3Al, when irradiated by neutrons. Therefore, it must be assumed that the neutron irradiation of Fe_3Al produces atomic rearrangements that are more extensive than can be accounted for by displaced atoms alone. Thus, the change in resistivity comes from a change in the degree of long range order. A thermal spike cannot cause the change in long range order, for it just excites the atoms in their lattice sites and does not give them enough energy to jump out of the lattice site.

A displacement spike is characterized by a large amount of energy being imparted to an atom in a lattice site. This energy will be transferred to the atom's neighbors which now become abnormally excited. If this imparted energy is large, the atoms will leave their lattice sites and take up interstitial positions. So by this process, the long range order could be disrupted.

With a replacement collision, the long range order can also be disrupted by a "wrong" mobile atom, which does not have enough energy to cause a displacement, but does have enough energy to substitute for a "right" atom and push the "right" atom into an interstitial position.

It should be pointed out that the vacancy/interstitial produced by a displacement or the interstitial produced by a replacement collision must be a metastable configuration at the elevated temperatures, for when the Fe_3Al was cooled to room temperature, the order parameter increased, thus indicating a tendency toward order at the lower temperatures. The vacancies are annihilated and the "right" atoms move back to the "right" sites.

This is evident when the long range order parameter calculated by Muto's relationship and by integrated intensity are campared(both in initially ordered and disordered states). Muto's relationship method of calculating long range order used the resistivities at the elevated temperatures. The long range order parameter calculated by integrated intensity was obtained at room temperature. The long range order parameter from integrated intensity is substantially larger than the one calculated from Muto's relationship. This definitely indicates that the point defects formed during irradiation at the elevated test temperature are annealed out on subsequent cooling.

The effect the temperature has on the resistivity, and thus the order, of Fe_3Al must be connected with the mobilities of the vacancies and interstitials already present and also on the vacancies and interstitials generated during irradiation. The temperature also increases the energy of atoms in the lattice sites thus making it easier for another atom to replace them.

As was stated earlier, the resistivity of the Fe_3Al at 300°C almost became constant. This could only happen if the vacancies annihilated equaled the number of vacancy/interstitial pairs produced and of the number of "right" atoms replaced equaled the number of "wrong" atoms replaced.

In this investigation, activation energies for Fe_3Al in initially ordered and initially disordered states were calculated(see appendix B). The activation energy for the initially ordered Fe_3Al as it moved toward disorder was 0.0417 eV and for the initially disordered Fe_3Al as it moved toward order was 0.0662 eV. These energies are substantially lower than normally determined activation energy. It must, therefore, be concluded that this is a pseudoactivation energy. Part of it being obtained from the elevated temperatures and part from the neutron irradiation.

CHAPTER VI

CONCLUSIONS

Resistivity measurements obtained in this investigation indicate that disordering increases by the production of displacement spikes and replacement collisions which disrupt the long range order that existed.

Long range order parameters calculated from Muto's relationship and integrated intensities from x-ray diffraction patterns show that vacancy/interstitial pairs and interstitials produced by replacement collisions are metastable at the elevated temperatures for the order is increased when the temperature is lowered.

Calculations of the activation energies for initially ordered and disordered Fe_3Al, after being irradiated, are pseudoactivation energies.

CHAPTER VII

RECOMMENDATIONS

Study of order-disorder in Fe_3Al at very low temperatures when neutron irradiated. The damage incurred by the Fe_3Al will then be solely radiation damage.

Neutron diffraction of neutron irradiated ordered and disordered Fe_3Al to determine better order parameters.

Annealing investigations after neutron irradiation of Fe_3Al to determine a true activation energy and better understanding of the nature of the point defects incurred during irradiation.

APPENDIX

APPENDIX A

Experimental Data

Ordered Fe_3Al 10 KW 200°C

Length of Specimen - 5.44 in. Width - 0.507 in.

Thickness - 0.039 in.

Time (hours)	Resistance (μohms)	Resistivity (μohm-cm)
0	11720	108.2
1	12700	117.2
2	13240	122.2
3	13400	124.0
4	13600	125.8
5	13760	127.4
6	13940	128.9
7	14100	130.4
8	14280	132.1
9	14420	133.4
10	14540	134.5

Ordered Fe_3Al 2 KW 100°C

Length of Specimen - 5.51 in. Width - 0.505 in.

Thickness - 0.038 in.

Time (hours)	Resistance (μohms)	Resistivity (μohm-cm)
0	10180	90.4
1	10520	93.1
2	10700	94.7
3	10820	95.7
4	10920	96.6
5	11000	97.3
6	11100	98.2
7	11220	99.3
8	11320	100.1
9	11440	101.2
10	11520	101.9

Ordered Fe_3Al 2 KW 150°C

Length of Specimen - 5.14 in. Width - 0.503 in.

Thickness - 0.038 in.

Time (hours)	Resistance (μ ohms)	Resistivity (μ ohm-cm)
0	10700	101.0
1	11080	104.6
2	11220	105.9
3	11360	107.2
4	11500	108.6
5	11600	109.7
6	11700	110.4
7	11820	111.6
8	11940	112.7
9	12040	113.7
10	12160	114.8

Ordered Fe_3Al 2 KW 200°C

Length of Specimen - 5.20 in. Width - 0.505 in.

Thickness - 0.039 in.

Time (hours)	Resistance (μohms)	Resistivity (μohm-cm)
0	11140	107.2
½	11380	109.5
1	11500	110.6
1½	11600	111.6
2	11660	112.2
3	11780	113.3
3½	11860	114.1
4	11920	114.7
4½	11960	115.1
5	12020	115.6
5½	12060	116.0
6	12120	116.6
6½	12180	117.2
7	12240	117.7
7½	12300	118.3
8	12360	118.9
8½	12440	119.7
9	12500	120.3
9½	12560	120.8
10	12620	121.4

Ordered Fe_3Al 2 KW 250°C

Length of Specimen - 4.67 in. Width - 0.505 in.

Thickness - 0.038 in.

Time (hours)	Resistance (μohms)	Resistivity (μohm-cm)
0	11500	120.1
1	11880	124.0
2	12060	125.9
3	12200	127.4
4	12340	128.8
5	12460	130.1
6	12580	131.3
7	12700	132.6
8	12800	133.6
9	12920	134.8
10	13040	136.1

Ordered Fe_3Al 2 KW 300°C

Length of Specimen - 5.76 in. Width - 0.506 in.

Thickness - 0.038 in.

Time (hours)	Resistance (μ ohms)	Resistivity (μ ohm-cm)
0	15700	133.1
1	16080	136.3
2	16320	138.3
3	16460	139.5
4	16560	140.4
5	16600	140.7
6	16620	140.9
7	16640	141.1
8	16660	141.2
9	16680	141.4
10	16700	141.6

Disordered Fe_3Al 2 KW 100°C

Length of Specimen - 5.25 in. Width - 0.510 in.

Thickness - 0.039 in.

Time (hours)	Resistance (μohms)	Resistivity (μohm-cm)
0	17000	154.9
1	15740	151.4
2	15500	149.2
3	15320	147.4
4	15180	146.1
5	15080	145.1
6	15000	144.3
7	14940	143.8
8	14880	143.2
9	14820	142.6
10	14780	142.1

Disordered Fe_3Al 2 KW 150°C

Length of Specimen - 4.90 in. Width - 0.510 in.

Thickness - 0.038 in.

Time (hours)	Resistance (μohms)	Resistivity (μohm-cm)
0	15400	154.8
1	15020	151.0
2	14740	148.1
3	14620	146.9
4	14540	146.1
5	14460	145.1
6	14380	144.5
7	14340	144.1
8	14280	143.5
9	14220	142.9
10	14180	142.5

Disordered Fe_3Al 2 KW 200°C

Length of Specimen - 5.51 in. Width - 0.506 in.

Thickness - 0.039 in.

Time (hours)	Resistance (μohms)	Resistivity (μohm-cm)
0	17040	154.5
1	16580	150.5
2	16280	147.8
3	16160	146.7
4	16060	145.8
5	15960	144.9
6	15900	144.3
7	15820	143.6
8	15760	143.1
9	15720	142.7
10	15680	142.4

Disordered Fe_3Al 2 KW 250°C

Length of Specimen - 5.20 in. Width - 0.503 in.

Thickness - 0.038 in.

Time (hours)	Resistance (μohms)	Resistivity (μohm-cm)
0	16600	155.0
1	16080	150.1
2	15820	147.7
3	15640	146.0
4	15500	144.7
5	15380	143.6
6	15320	143.0
7	15280	142.7
8	15260	142.5
9	15240	142.3
10	15220	142.1

Disordered Fe_3Al 2 KW 300°C

Length of Specimen - 5.72 in. Width - 0.509 in.

Thickness - 0.039 in.

Time (hours)	Resistance (μohms)	Resistivity (μohm-cm)
0	17500	154.2
1	16800	148.0
2	16480	145.2
3	16260	143.3
4	16200	142.7
5	16140	142.2
6	16100	141.9
7	16080	141.7
8	16060	141.5
9	16040	141.3
10	16040	141.3

APPENDIX B

Activation Energy Data

To calculate the activation energy for the initially ordered Fe_3Al going towards the disordered state and the initially disordered Fe_3Al going toward the ordered state, the change in resistivity($\Delta\rho$) vs. $1/T^oK$ was plotted. Figure 30 is the curve for the initially ordered Fe_3Al going toward the disordered. $\Delta\rho$ was obtained by subtracting the initial resistivity from the resistivity after 3 hours of irradiation for each temperature. The $\Delta\rho$ for 300°C was not taken due to the smaller change when the resistivity became constant. Figure 31 is the curve for the initially disordered Fe_3Al going toward the ordered state. Here the resistivity measured after 1 hour of irradiation was subtracted from the initial resistivity(at zero flux).

If two points are taken on the curve, such as ρ_1 and ρ_2, the activation energy can be solved for by using the following:

$$\frac{\rho_1}{\rho_2} = \frac{A \exp -E_a/kT_1}{A \exp -E_a/kT_2}$$

The constant A cancels out and $\rho_1/\rho_2 = \exp -E_a/k(1/T_1 - 1/T_2)$ is left. Since we know the value of ρ_1 and ρ_2 and the values of T_1 and T_2, E_a can be calculated.

Sample Calculations

$$2.95/6.20 = \exp -E_a/k(1/376 - 1/576)$$

$$\ln(.492) = -E_a/k(.925 \times 10^{-3}/^oK)$$

$$\frac{(-.709)(1.38 \times 10^{-16}\ erg/^oK)}{(.925 \times 10^{-3}/^oK)(1.602 \times 10^{-12} erg/eV)} = -E_a$$

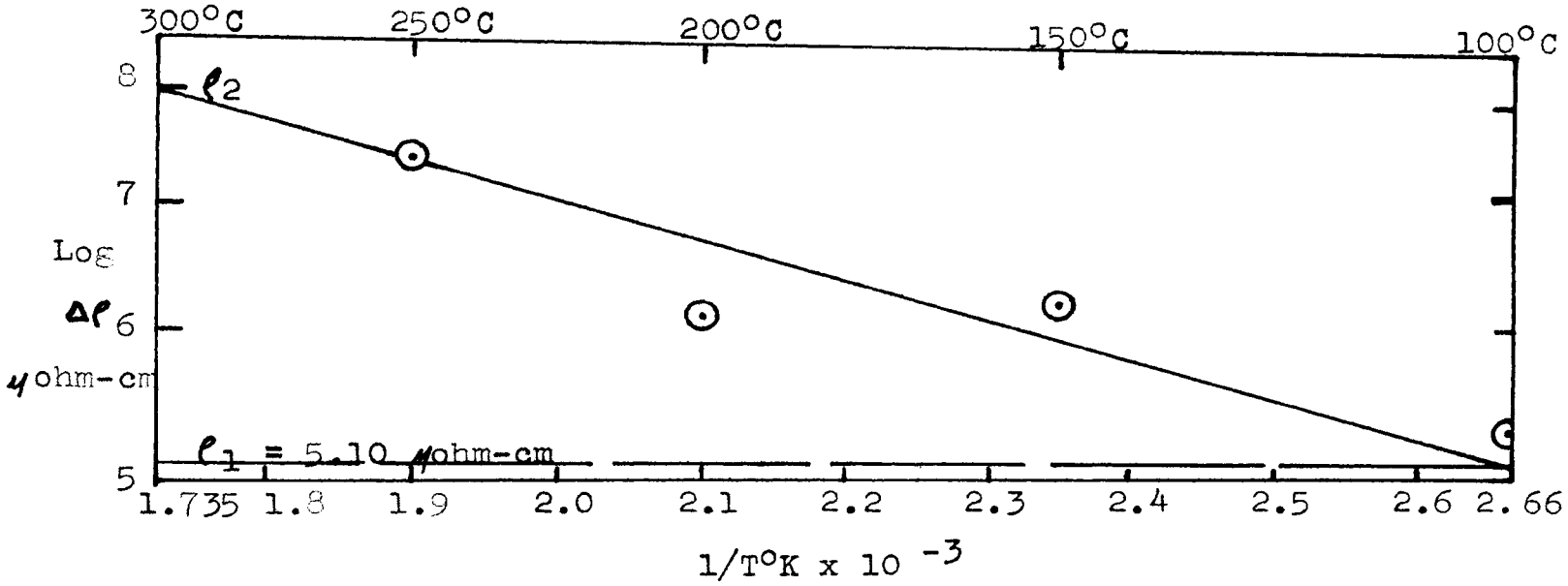

Change in resistivity vs. 1/T°K for initially ordered Fe_3Al going toward the disordered state.

Figure 30.

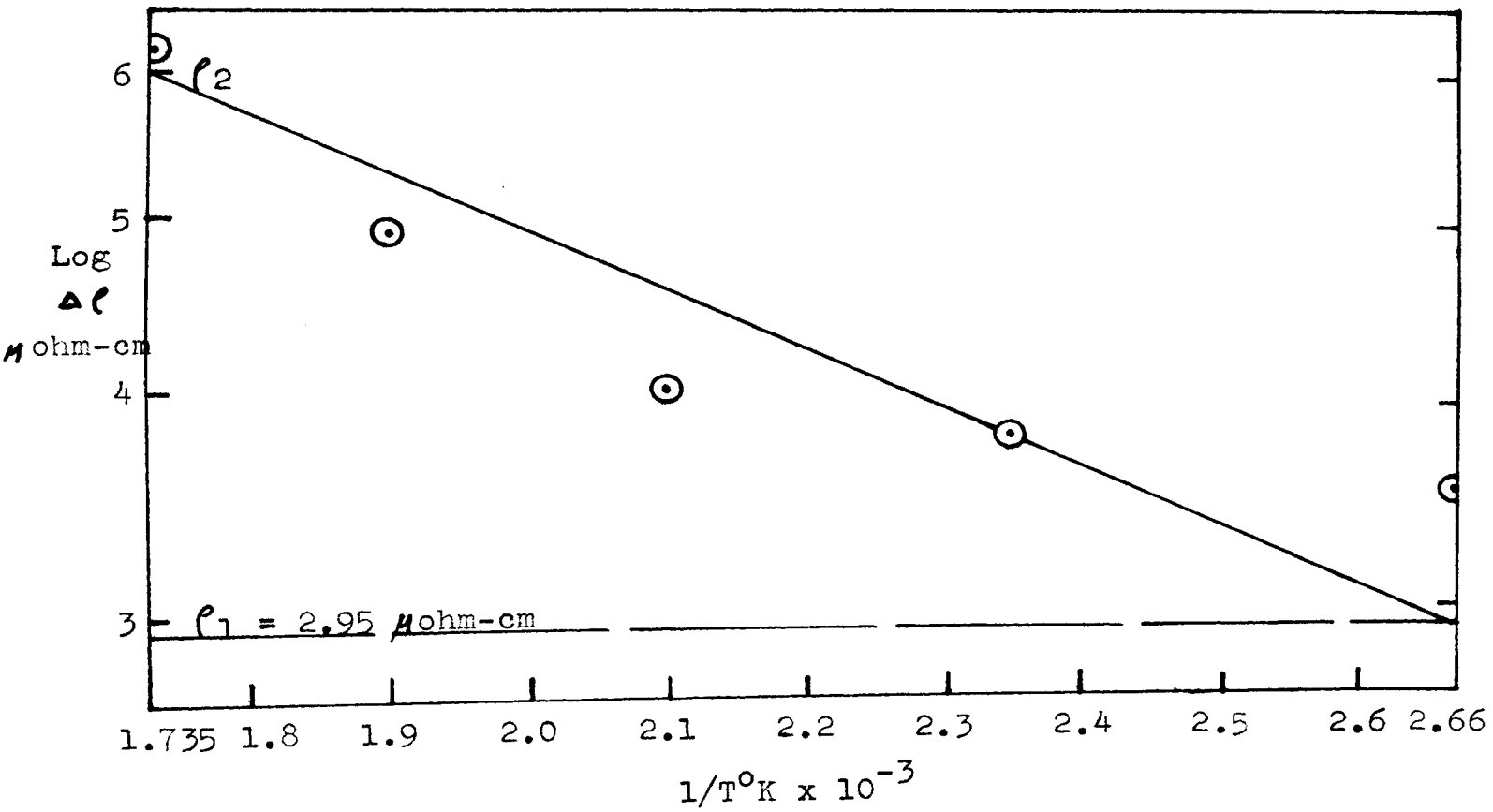

Change in resistivity vs. 1/T°K for initially disordered Fe_3Al going toward the ordered state.

Figure 31.

$$0.0662 \text{ eV} = E_a$$

This was the value obtained for the initially disordered Fe_3Al going toward the ordered state. By using the same process, an activation energy of 0.0417 eV can be obtained for the initially ordered Fe_3Al going toward the disordered state.

BIBLIOGRAPHY

(1) BENNET, W. D. (1952) Some effects of order-disorder in iron-aluminum alloys. Journal of the Iron and Steel Institute. 171-172 p. 372

(2) BETTS, B. (1964) Personal communication.

(3) BILLINGTON, D. S. and J. H. CRAWFORD JR. (1961) Radiation damage in solids. Princeton University Press, Princeton, New Jersey. 450 p.

(4) BRADLEY, A. and A. JAY (1932) Proc. Roy. Soc. A136, p. 210.

(5) BRAGG, W. L. and E. J. WILLIAMS (1935) The effect of thermal agitation on atomic arrangement in alloys-II. Proc. Roy. Soc. A151, p. 540.

(6) BRINKMAN, J. A. (1956) Production of atomic displacements by high-energy particles. American Journal of Physics, 24, p. 246-267.

(7) BRINKMAN, J. A. (1955) Effects of fission fragments on radiation damaged metals. U.S.A.E.C. Report, No. NAA-SR-262.

(8) COTTRELL, A. H. (1959) Effect of nuclear radiation on engineering materials. Journal of British Nuclear Energy Conference, 5-6, p. 64-76.

(9) COTTRELL, A. H. (1958) Effects of neutron irradiation on metals and alloys. Journal of British Nuclear Energy Conference, 3, p. 50-67.

(10) DIENES, G. J. and G. H. VINEYARD (1957) Radiation effects in solids. Interscience Publishing Inc., New York, Vol. II, 226 p.

(11) DUGDALE, R. A. and A. GREEN (1954) Some ordering effects in Cu_3Au at about 100°C. Phil. Mag., 45, p. 163.

(12) ELCOCK, E. (1956) Order-disorder phenomena. Methuen's Monographs on Physical Subjects, John Wiley and Son Inc., New York.

(13) GLEN, J. W. (1955) A survey of irradiation effects in metals. Advanc. Phys., 4, p. 381.

(14) HANSEN, M. and K. ANDERKO (1958) Constitution of Binary alloys. McGraw-Hill, New york.

(15) KINCHIN, G. H. and R. S. PEASE (1954) the mechanism of the irradiation disordering of alloys. Journal of Nuclear Engineering, 1-2, p. 200-202.

(16) LEIGHLY, H. P. JR. (1965) Personal communication.

(17) LIPSON, H. (1950) Order-disorder changes in alloys. Progress in Metal Physics, 2, p. 1-50.

(18) LOMER, W. M. (1954) Diffusion coefficients in copper under fast neutron irradiation. A.E.R.E. Report, No. T/R 1540.

(19) LOMER, W. M. and A. H. COTTRELL (1955) Annealing of point defects in metals and alloys. Phil. Mag., 46, p. 711.

(20) MCQUEEN, H. and G. KUCZYNSKI (1959) Trans. AIME, 215, p. 619.

(21) MUTO, T. and Y. TAKAGI (1955) The theory of order-disorder transitions in alloys. Solid State Physics, Vol. 1, Academic Press Inc., New York,

(22) NABARRO, F. R. N. (1948) Deformation of crystals by the motion of single ions. Report of Conference on Strengths of Solids, p. 75.

(23) RAUSCHER, G. P. JR. (1962) A study of the superlattice transformations in iron-aluminum alloys. Thesis, University of Denver, 71 p.

(24) ROSWELL, A. E. and A. S. NORWICK (1953) Decay of lattice defects frozen into a silver-zinc alloy by quenching. Trans. Amer. Inst. Min. Engrs., 197, p. 1259.

(25) SAENKO, G. P. (1962) Effects of neutron irradiation on the ordered alloy Fe_3Al. U.S.A.E.C. Report, AEC-TR-5245. 15p.

(26) SEITZ, F. and J. S. KOEHLER (1956) Displacement of atoms during irradiation. Solid State Phys., 2, p. 305.

(27) SIEGEL, S. (1949) Effects of neutron bombardment on order in the alloy Cu_3Au. Phys. Rev., 75, p. 1823.

(28) SYKES, C. and J. BAMPFYLDE (1934) J. Iron and Steel Inst., 130, p. 389.

(29) TAYLOR, A. and R. JONES (1958) J. Phys. Chem. Solids, 6, p. 16.

(30) Neutron Cross Sections (1958) BNL 325, second edition, Brookhaven National Laboratory, Upton, New York.

VITA

The author was born in St. Louis, Missouri on September 18, 1940. In July 1962, he received the degree of Bachelor of Science in Metallurgical Engineering from the Missouri School of Mines and Metallurgy.

In September 1964, after two years in the United States Army, he returned to the University of Missouri at Rolla to begin work on the Master of Science degree in Metallurgical Engineering.